2015-09

LOCALIZATION AND TRACKING OF 4G COGNITIVE RADIO

Lee, Wei San

Monterey, California. Naval Postgraduate School

NAVAL POSTGRADUATE SCHOOL

MONTEREY, CALIFORNIA

THESIS

LOCALIZATION AND TRACKING OF 4G COGNITIVE RADIO

by

Wei San Lee

September 2015

Thesis Co-Advisors: Weilian Su
Tri T. Ha
Ric Romero

Approved for public release; distribution is unlimited

THIS PAGE INTENTIONALLY LEFT BLANK

REPORT DOCUMENTATION PAGE

Form Approved OMB No. 0704–0188

1. AGENCY USE ONLY *(Leave blank)*	**2. REPORT DATE** September 2015	**3. REPORT TYPE AND DATES COVERED** Master's Thesis

4. TITLE AND SUBTITLE
LOCALIZATION AND TRACKING OF 4G COGNITIVE RADIO

5. FUNDING NUMBERS

6. AUTHOR(S) Lee, Wei San

7. PERFORMING ORGANIZATION NAME(S) AND ADDRESS(ES)
Naval Postgraduate School
Monterey, CA 93943-5000

8. PERFORMING ORGANIZATION REPORT NUMBER

9. SPONSORING /MONITORING AGENCY NAME(S) AND ADDRESS(ES)
N/A

10. SPONSORING/MONITORING AGENCY REPORT NUMBER

11. SUPPLEMENTARY NOTES The views expressed in this thesis are those of the author and do not reflect the official policy or position of the Department of Defense or the U.S. Government. IRB Protocol number ____N/A____.

12a. DISTRIBUTION / AVAILABILITY STATEMENT
Approved for public release; distribution is unlimited

12b. DISTRIBUTION CODE

13. ABSTRACT (maximum 200 words)

The 4G network provides a significant improvement in performance, but service providers are still faced with the annual increase in usage of cell phones and wireless devices. Spectrum efficiency is the most prominent issue in handling the high number of users. The cognitive radio is capable of changing its transmission and/or reception parameters according to the demands of the network. In the 4G network, the cognitive radio is seen as a solution to spectrum efficiency. With the high number of users, it also means that there is a need to effectively localize and track the 4G cognitive radio (4G-CR) signal for various purposes such as urban environment warfare, national security, surveillance, intelligence, and emergency rescue.

The localization errors from previous proposed methods of time-difference-of-arrival (TDOA) measurements were analyzed in this thesis. The localization errors obtained are close to the differential-distance errors derived from the TDOA measurement algorithms. In addition, the localization of 4G-CR requires an adaptive tracking method, which is also discussed in this thesis.

14. SUBJECT TERMS
cognitive radio, 4G network, wireless sensor network, localization error, adaptive tracking

15. NUMBER OF PAGES
87

16. PRICE CODE

17. SECURITY CLASSIFICATION OF REPORT	**18. SECURITY CLASSIFICATION OF THIS PAGE**	**19. SECURITY CLASSIFICATION OF ABSTRACT**	**20. LIMITATION OF ABSTRACT**
Unclassified	Unclassified	Unclassified	UU

NSN 7540–01-280-5500

Standard Form 298 (Rev. 2–89)
Prescribed by ANSI Std. 239–18

THIS PAGE INTENTIONALLY LEFT BLANK

Approved for public release; distribution is unlimited

LOCALIZATION AND TRACKING OF 4G COGNITIVE RADIO

Wei San Lee
Civilian, ST Electronics, Singapore
B.Eng. (EE), National University of Singapore, 2008

Submitted in partial fulfillment of the
requirements for the degree of

MASTER OF SCIENCE IN ELECTRICAL ENGINEERING

from the

NAVAL POSTGRADUATE SCHOOL
September 2015

Author: Wei San Lee

Approved by: Weilian Su
Thesis Advisor

Tri T. Ha
Co-Advisor

Ric Romero
Co-Advisor

Clark R. Robertson
Chair, Department of Electrical and Computer Engineering

THIS PAGE INTENTIONALLY LEFT BLANK

ABSTRACT

The 4G network provides a significant improvement in performance, but service providers are still faced with the annual increase in usage of cell phones and wireless devices. Spectrum efficiency is the most prominent issue in handling the high number of users. The cognitive radio is capable of changing its transmission and/or reception parameters according to the demands of the network. In the 4G network, the cognitive radio is seen as a solution to spectrum efficiency. With the high number of users, it also means that there is a need to effectively localize and track the 4G cognitive radio (4G-CR) signal for various purposes such as urban environment warfare, national security, surveillance, intelligence, and emergency rescue.

The localization errors from previous proposed methods of time-difference-of-arrival (TDOA) measurements were analyzed in this thesis. The localization errors obtained are close to the differential-distance errors derived from the TDOA measurement algorithms. In addition, the localization of 4G-CR requires an adaptive tracking method, which is also discussed in this thesis.

THIS PAGE INTENTIONALLY LEFT BLANK

TABLE OF CONTENTS

THIS PAGE INTENTIONALLY LEFT BLANK

LIST OF FIGURES

THIS PAGE INTENTIONALLY LEFT BLANK

LIST OF TABLES

THIS PAGE INTENTIONALLY LEFT BLANK

LIST OF ACRONYMS AND ABBREVIATIONS

4G	4th generation
4G-CR	4th generation cognitive radio
BS	Base station
CPE	Customer premise equipment
CR	Cognitive radio
CRN	Cognitive radio network
CRS	Cognitive radio system
DARPA	Defense Advanced Research Projects Agency
DDPA	Double-differential phase algorithm
DA-DDPA	Data-aided double-differential phase algorithm
DM	Decision maker
ECSS	Enhanced cooperative spectrum sensing
EL-FFT.SA	Early-late FFT sampling algorithm
FFT	Fast Fourier transform
FH	Frequency hopping
GPS	Global positioning system
LTE	Long-term evolution
MAC	Medium access control
OFDM	Orthogonal frequency-division multiplexing
OFDMA	Orthogonal frequency-division multiple access
RF	Radio frequency
PU	Primary user
QAM	Quadrature amplitude multiplexing
QPSK	Quadrature phase-shift keying
RMS	root-mean-squared
SCH	Superframe control header
SM	Spectrum manager
SSA	Spectrum-sensing automaton
SNR	Signal-to-noise ratio
SSF	Spectrum-sensing function

SU	Secondary user
TDOA	Time-difference-of-arrival
TV	Television
WANN	Wireless adaptive node network
WiMax	Worldwide interoperability for microwave access
WRAN	Wireless regional area network

ACKNOWLEDGMENTS

I want to thank my advisors, Professor Weilian Su, Professor Tri Ha and Professor Ric Romero for their guidance. They have also provided valuable advice for my thesis. Special thanks to Professor Ha who also shared his life philosophies during every thesis meeting.

I also want to thank my parents, my sister and my brothers for their moral support.

I am thankful for my housemates, Tammi and Jeanette, who are both fantastic cooks.

Finally, I want to thank Eugene, for always being so patient and encouraging. I am glad to have him by my side during all this time.

THIS PAGE INTENTIONALLY LEFT BLANK

I. INTRODUCTION

A. BACKGROUND

1. 4G (4th Generation) Network

According to International Telecommunication Union (ITU), LTE-Advanced (Long-Term Evolution-Advanced) and WiMAX (Worldwide Interoperability for Microwave Access) Release 2.0 are officially designated as IMT-Advanced (International Mobile Telecommunications-Advanced) systems [1]. IMT-Advanced systems are not termed as 4G so as to reduce confusion with commercially marketed 4G networks which are actually 3G+ networks; however, in this thesis, 4G networks are referred as IMT-Advanced systems.

The 4G networks provide improvements in spectrum efficiency so as to be able to support more users at higher data rates per radio channel. The architecture is fully packet-based with lower overall latency [1]. The improved radio resource management and control has enhanced quality-of-service. There are new capabilities such as wideband radio channels and multiple-input multiple-output (MIMO) which can be used to improve communication performance.

The commercial 4G telecommunication network, LTE-Advanced, also has the advantage of having one global standard [2], which increases interoperability and results in quicker responses for public safety rescue operations. Based on post analyses of natural disaster and terrorist attacks, the most significant hindrance to initial rescue response is the lack of interoperability between communication assets of rescue organizations and the network of the affected area [3].

2. Cognitive Radio System

The cognitive radio system (CRS) is defined on the ITU website as “a radio system employing technology that allows the system to obtain knowledge of its operational and geographical environment, established policies and its internal state” [4]. With the acquired knowledge, the radio system is able to “dynamically and autonomously

adjust its operational parameters and protocols" so it can "achieve predefined objectives" [4].

One feature of CR environment is that there are two types of users, namely primary and secondary. The primary users (PUs) are authorized to use the frequency spectrum in a specific geographical area, and the primary user network is likely to have excess resources available on the spectrum. The secondary user (SU) utilizes the spectrum in an opportunistic manner and has the responsibility of avoiding interference with the primary users [5].

3. Orthogonal Frequency-Division Multiplexing (OFDM)

OFDM is currently employed in WiFi, WiMAX (Worldwide Interoperability for Microwave Access), WRAN (wireless regional area network) and the cellular standard LTE. OFDM is considered to be an excellent multiplexing technique for common telecommunication modulation formats such as QPSK and QAM due to its robustness in multipath fading channels, high spectral efficiency and dynamic spectrum use [6]. OFDM allows the subcarriers to be turned on or off in accordance to available spectrum availability; hence, it is a good modulation technique for the CR [6].

4. 4G Cognitive Radio (4G-CR)

In this thesis, the 4G cognitive radio (4G-CR) is defined as a cognitive radio system in a 4G network which utilizes orthogonal frequency-division multiplexing (OFDM).

5. Issues and Challenges

Although there is an expected significant improvement in performance, 4G networks are still faced with the annual increase in usage of cell phones and wireless devices. Spectrum efficiency is the most prominent issue in handling the large number of users. The CRS is a potential solution to spectrum efficiency because it is capable of detecting spectrum availability and adjusting its transmission and/or reception parameters accordingly [3], [6]. The CRS is considered to provide spectrum-loading flexibility [3] in the event of unusual load conditions, and it is seen as a means of providing service

flexibility when operating in a heterogeneous communication environment where there are several service providers or radio standards such as WiMAX or 3G/4G [2].

With the use of CRs in a 4G network, there is a need to effectively localize and track a 4G-CR target for various purposes such as urban environment warfare, national security, surveillance, intelligence, emergency rescue. The localization of CR is even more essential when adversaries and terrorists can use CRs for cyber warfare [5]. The challenge is the inherent dynamic nature of a 4G-CR signal. The 4G-CR target cannot solely be localized using conventional localization methods as there is a constant change in spatial, frequency and temporal parameters. There has been very little work on localization of CR [7].

B. PURPOSE OF RESEARCH AND RELATED WORK

1. Passive Localization Using Time-Difference-of-Arrival (TDOA)

Passive localization is advantageous to users because of the low cost and power requirements. With no transmission of a radio frequency (RF) signal, the power requirement is low and costs are kept low. Passive localization is relatively faster than active localization as there is no wait time required for returned signals.

Time-difference-of-arrival (TDOA) localization methods are beneficial as there is no need for time synchronization between transmitters and receivers. Past work has identified the pilot symbols in an OFDM signal as the most important parameter for localization [8]. There are three proposed TDOA algorithms to localize emitters using static and passive sensors. The pros and cons of the three methods, including the expected TDOA errors, were presented in [8].

The localization method using geostationary satellites has been analyzed in detail, and the results are promising [9], [10]. A Monte Carlo-based method and a non-linear least-squares framework were compared for localization, and the non-linear least-squares method with at least three sensors was recommended in [11]; hence, the least-squares method in [9] is used for the error analysis in this thesis. An analysis of sensor-position errors on source localization is provided in [12]. The sensor-position error is included in the error analysis and effects observed in this research are discussed in Chapter IV.

Previous work is continued in this thesis by analyzing the localization error based on the expected TDOA errors in [8] and sensor-position errors.

2. Tracking of 4G-CR

The issue of spectrum efficiency motivated the study of utilizing the white spaces of the licensed spectrum while maintaining low probability of interference. The Institute of Electrical and Electronics Engineers (IEEE) standard 802.22 [13] is a standard for WRAN and utilized CR techniques to use the unused portion of the television (TV) frequency spectrum without causing interference to the primary operation of digital TV broadcast. The unused portion of the RF spectrum are called white spaces. In a 4G network, wireless devices can possess CR capability similar to that in IEEE 802.22 devices, increasing the spectrum efficiency of the 4G networks. Both the spectrum-sensing function (SSF) of IEEE 802.22 and the localization methods of CRs are discussed in Chapter V. There are suggestions for strategies in Chapter VI to track the 4G-CR signals for the purposes of emergency rescue or surveillance.

The proposed method in [14] is used to localize secondary users (SU) based on their measurement of primary user (PU) signals in the TV spectrum while the extended semi-range based method to localize a CR is provided by [5]. In a 4G network, the secondary user target can be detected using an external wireless sensor network. This scenario is adopted for the thesis.

3. Objectives

There are two objectives for this thesis research. The first is to continue the work from [8], where an error analysis is to be conducted based on the mathematical results from previous TDOA localization methods of a 4G OFDM signal. The second objective is to propose an adaptive localization method for 4G-CR, as the current localization methods are insufficient to track the 4G-CR continuously.

With the above objectives, this thesis is a contribution to the study of localizing and tracking 4G-CR signals and, particularly, OFDM signals.

C. RESEARCH WORK OUTLINE

1. Part 1: TDOA Localization-Error Analysis

The investigation of the localization error with the use of time-difference-of-arrival (TDOA) on static sensors is included in Chapters III and IV. The error analysis provides insight into the accuracy of the new TDOA methods proposed in [8] for OFDM signals. The effect of sensor-position error on localization error is also analyzed. The mathematical model is first presented, a Matlab simulation of the model is conducted, and the results are analyzed. There is also a discussion on practical implications.

2. Part 2: Adaptive Localization and Tracking Strategies

The localization of 4G-CR signal is challenging due to changes in spatial, frequency and temporal parameters. Current localization methods are insufficient to continuously track the 4G-CR signal. The discussion of cognitive radio capabilities in IEEE 802.22 are included in Chapter V, which are adopted in the conceptualization of the adaptive localization method for 4G-CR in Chapter VI.

THIS PAGE INTENTIONALLY LEFT BLANK

II. PREVIOUS WORK

A. GOALS OF THE STUDY

The previous work in [8] consists of a study of the 4G-CR with the following goals:

a) identify parameters in the adaptive frequency hopping (FH)-OFDM-based waveform and
b) devise methods to effectively localize and track 4G-CR radios.

The study successfully identified the pilot symbol as the most important parameter for localization of the 4G-CR signals. Three methods of TDOA localization were proposed at the end of the study, and the expected TDOA error uncertainty forms the basis of research in this thesis.

B. FINDINGS FROM THE STUDY

1. Methods of TDOA Measurement

The pilot symbol carries reference information in the OFDM waveform for demodulation. This information can be leveraged for localization purpose. The three main methods of TDOA measurement utilize the pilot symbol as part of the measurement.

a) Single-pilot subcarrier measurement (differential-phase method)

This differential-phase method uses two synchronized sensors, which detect the pilot symbol from the emitter. Each sensor detects the pilot symbol, and the phase difference of the two symbols is used to calculate the TDOA relative to the reference time.

This measurement technique requires the TDOA to be much smaller than the symbol time; hence, the emitter must be close to the sensors, or the distance difference from the emitter to the sensors has to be shorter so that the frequency-time constraint is satisfied. The other drawback is phase-ambiguity, which is not practical for high data rate signals.

b) Two-pilot subcarrier measurement (double-differential phase method)

This double-differential phase method is based on the measurement of two pilot symbols from two subcarriers at two different frequencies. If the two symbols are identical, the phase difference at emitter's transmission time is 0 degrees. If the symbols are different, then it is necessary for the sensors to possess knowledge of the phase difference at emitter's transmission time.

The phase-ambiguity problem is still present in this method; however, the time constraint is less restrictive than for the first method. This is because TDOA is inversely proportional to the difference in carrier frequencies between the two subcarriers. This method is more practical for current high speed networks.

c) Direct-timing measurement

The double-differential phase method does not have phase-ambiguity when the TDOA is much smaller than an OFDM period *T*, which is the subcarrier symbol time.

The sensors have an existing mechanism for reference synchronization timing t_0. To derive the coarse estimation of the TDOA, the sensors compare the frame synchronization timing that each obtains and compares it with t_0. The frame synchronization timing at every sensor is obtained via the trained OFDM symbol sequence in the preamble of the data frame. The location of an OFDM symbol in the data frame is obtained relative to the frame synchronization timing. The fine estimation of the TDOA can be obtained via one or more pilot symbols in the current OFDM symbol.

This method works with one or more pilot subcarriers and does not have any phase-ambiguity. The drawback is that there is a need for precise reference timing between the sensors. The reference synchronization timing is also subject to the same timing jitters as the frame synchronization timing. This further increases the TDOA error.

2. Proposed Algorithms for TDOA Measurement

The three proposed algorithms in [8] are:

a) Early-late FFT sampling algorithm (EL-FFT.SA)

This method uses the direct-timing measurement and aims to find the minimum Euclidean distance between the co-phased sampled pilot symbols at various FFT sample timings to the known pilot symbol stored at the sensor.

b) Double-differential phase algorithm (DDPA)

This algorithm utilizes the double-differential phase method. It does not require precise synchronized reference timing because the TDOA is calculated from the difference in phases between two pilot symbols obtained from two sensors. The disadvantage is that phase-ambiguity still exists if the sensors are located far from the emitter or from each other. Since the FFT sampling timing and the time-of-arrival can be derived from this algorithm, EL-FFT.SA can be used as a supplement to DDPA.

c) Data-aided double-differential phase algorithm (DA-DDPA)

This is an alternative to DDPA as it extends the range ambiguity. An extended range ambiguity means that the maximum unambiguous distance between sensor and emitter is extended. The range ambiguity is linearly proportional to the frequency separation between two subcarriers. A larger frequency separation increases the maximum unambiguous range. In a typical OFDM signal, the frequency separation between two adjacent pilot subcarriers is more than the frequency separation between two adjacent subcarriers. Instead of using phase difference between two pilot subcarriers, the data subcarrier that is adjacent to a pilot subcarrier is utilized in this algorithm. Although DA-DDPA can extend the range of sensors, there is a disadvantage of higher vulnerability to error due to lower signal-to-noise ratio (SNR) of the data symbol as compared to the higher pilot-to-noise ratio.

3. Initial Assessment of The Three Proposed Algorithms

The EL-FFT.SA method has no phase-ambiguity and works with one or more pilot subcarriers; however, it requires precise, synchronized reference timing among the sensors. The FFT sampling time must be kept the same and requires a clock time that is synchronized with the OFDM clock.

The DDPA works with at least two pilot subcarriers but still has the phase-ambiguity problem. The advantage is that it does not require a precise synchronized reference time among the sensors and that the FFT sampling time does not need to be kept the same.

The DA-DDPA also has phase-ambiguity but allows a larger TDOA range; however, it is more susceptible to noise. Similar to DDPA, it does not require a precise, synchronized reference time among the sensors, and the FFT sampling time does not need to be kept the same.

4. Error Analysis of the Three Proposed Algorithms

a) Early-late FFT sampling algorithm (EL-FFT.SA)

The conclusion from the mathematical analysis is that there is a quantization error inherent in this method. A higher sampling rate reduces quantization error but increases the bandwidth and noise power. The increase in bandwidth and noise power reduces the SNR and can cause a misdetection of the true pilot sample. Since there is precise, synchronized reference timing, there is no phase-ambiguity. The performance of this algorithm depends on the quantization noise and timing jitter of the reference timing. The average TDOA error is expected to be less than 20.0 m.

b) Double-differential phase algorithm (DDPA)

There is no quantization error in this method because the differential-phase is used instead of the absolute phase. There is also no timing jitter error because TDOA is calculated from differential phases. Although precise synchronized reference timing is not required, phase-ambiguity is present in this method. The average TDOA error is expected to be less than 20.0 m.

c) Data-aided double-differential phase algorithm (DA-DDPA)

Similar to DDPA, there is no quantization error or timing jitter error. DA-DDPA is an alternative to DDPA as its range is extended with phase-ambiguity having a smaller impact on the result. Performance depends on the SNR of data subcarriers, which is about 7 to 10 dB lower than that of pilot subcarriers. In general, the TDOA root-mean-squared

(RMS) error is larger than that of DDPA; however, if the OFDM waveform has a large number of pilot subcarriers and small pilot subcarrier frequency spacing, this method can achieve the same performance as DDPA. The TDOA error is expected to be less than 90 m but, under certain circumstances, can achieve an error of less than 20.0 m.

C. RELATED WORK

With the expected TDOA error from the three proposed TDOA measurement methods, the localization-error analysis is discussed in Chapters III and IV.

THIS PAGE INTENTIONALLY LEFT BLANK

III. TDOA LOCALIZATION-ERROR ANALYSIS

In this chapter, the localization-error analysis and numerical results from the Matlab simulation are discussed. The modeling and simulation approach is discussed in this chapter, while the Matlab simulation results are presented in Chapter IV.

A. INTRODUCTION

The localization error was initially intended to investigate the use of TDOA method on static emitters and sensors; however, due to the high usage of drones for localization, part of the analysis was extended to include sensors more than 300 m in height. The error analysis is to provide insight into the accuracy of the new TDOA methods proposed in [8].

The differential-distance error uncertainty in [8] is +/-20 m, and this is used as the baseline for the localization-error analysis. As sensor-position error is predicted to contribute to localization error, it is also incorporated in the error analysis.

The modeling of the error analysis identifies the input variables and the coordinate system used in the mathematical model.

B. MODELING PROCESS

The model is such that there are *n* passive sensors and one emitter. The objective is to calculate the emitter-position error given certain input parameters. It is assumed that the true sensor position and true emitter position are known. The factors which affect the emitter-position error are identified and are used as input variables. The changes in the simulation model included the coordinate system and the least-squares solution.

1. Input Variables

The factors which affect the emitter-position error are categorized into primary and secondary types. These factors are used as input variables.

a. Primary Variables

The main goal of the error analysis is to study the effects of the primary input variables on the error in emitter position (Δx_e, Δy_e, Δz_e). The following are the primary variables, where $i, j = 1,2,\ldots, n$ and n represents number of sensors:

a) TDOA error ($\Delta\tau_{ij}$) or differential-distance error ($c\Delta\tau_{ij}$) and
b) sensor-position error (Δx_i, Δy_i, Δz_i).

b. Secondary Variables

The secondary variables can influence emitter-position error and are:

a) altitude of sensors ($h_i, i = 1, 2, \ldots n$),
b) range between emitter and sensors ($\|r_e - r_i\|, i = 1, 2, \ldots, n$), and
c) number of sensors (n).

2. Changes in the Modeling

The coordinate system and least-squares solution are two changes to the simulation model considered. The final model utilized the geocentric 3D Cartesian coordinate system and the modified least-squares solution.

a. Coordinate System

The type of coordinate system is also considered in the model. Initially, the three-dimensional (3D) Cartesian coordinate system with its origin at the emitter was used in the model; however, due to poor estimation of the earth surface, it was changed to a geocentric 3D Cartesian coordinate system with its origin at the center of Earth.

b. Modified Least-Squares Solution

The initial least-squares solution does not yield the best estimate for emitter-position error; hence, the least-squares solution was modified to make the estimate more accurate. The details of the two solutions are discussed further in the mathematical model.

The initial least-squares method did not provide a good estimate of the localization error due to the inherent characteristics of the geocentric coordinate system.

The contribution of error in the *z*-coordinate is relatively smaller than that for the *x*-coordinate and *y*-coordinate. The coordinates of sensors or emitters (*x*, *y*, *z*) are determined from the altitude *h*, longitude θ_L, and latitude θ_l according to

$$x = (R+h)\cos\theta_L \cos\theta_l, \tag{3.1}$$

$$y = (R+h)\sin\theta_L \cos\theta_l, \tag{3.2}$$

and

$$z = (R+h)\sin\theta_l. \tag{3.3}$$

It can be observed in Table 1 that the magnitude of *z* is significantly smaller when near the equator. At latitude five degrees North, *z* is 12% that of *z* at latitude 45 degrees North.

Table 1. Latitude effects on *x*, *y*, and *z*-coordinates.

GPS coordinates			***x, y, z-coordinates***		
Latitude θ_l	**Longitude** θ_L	**Altitude** ***h***	***x***	***y***	***z***
45˚N	150˚E	200 m	−3905833	2255034	4510068
10˚N	150˚E	200 m	−5439766	3140650	1107562
5˚N	150˚E	200 m	−5502663	3176964	555896

C. MATHEMATICAL MODEL

1. TDOA Equation

The distance between sensor *i* and the emitter is

$$\|\mathbf{r}_e - \mathbf{r}_i\| = \sqrt{(x_e - x_i)^2 + (y_e - y_i)^2 + (z_e - z_i)^2}, \tag{3.4}$$

where $\mathbf{r}_e$ is emitter position vector, $\mathbf{r}_i$ is sensor *i* position vector and *i* = 1,2,…*n* for *n* sensors. The differential-distance between sensor *i* and sensor *j* is

$$\left\|\boldsymbol{r}_e-\boldsymbol{r}_i\right\|-\left\|\boldsymbol{r}_e-\boldsymbol{r}_j\right\|=\sqrt{\left(x_e-x_i\right)^2+\left(y_e-y_i\right)^2+\left(z_e-z_i\right)^2}-\sqrt{\left(x_e-x_j\right)^2+\left(y_e-y_j\right)^2+\left(z_e-z_j\right)^2},$$
$$i,j=1,2,...,n;\quad i\neq j. \tag{3.5}$$

The differential-distance is equivalent to

$$c\tau_{ij}=\left\|\boldsymbol{r}_e-\boldsymbol{r}_i\right\|-\left\|\boldsymbol{r}_e-\boldsymbol{r}_j\right\|, \tag{3.6}$$

where c is the speed of light, and τ_{ij} is the TDOA between sensor i and sensor j. Substituting (3.5) into (3.6), we get the TDOA as

$$\tau_{ij}=\frac{1}{c}\sqrt{\left(x_e-x_i\right)^2+\left(y_e-y_i\right)^2+\left(z_e-z_i\right)^2}-\frac{1}{c}\sqrt{\left(x_e-x_j\right)^2+\left(y_e-y_j\right)^2+\left(z_e-z_j\right)^2}. \tag{3.7}$$

2. TDOA Error Equations

The partial differentiation of τ_{ij} with respect to x_e, y_e, and z_e gives the TDOA error

$$\Delta\tau_{ij}=\frac{\partial\tau_{ij}}{\partial x_e}\Delta x_e+\frac{\partial\tau_{ij}}{\partial y_e}\Delta y_e+\frac{\partial\tau_{ij}}{\partial z_e}\Delta z_e,\quad i,j=1,2,...,n;\quad i\neq j, \tag{3.8}$$

and the partial derivatives are

$$\frac{\partial\tau_{ij}}{\partial x_e}=\frac{1}{c}\frac{x_e-x_i}{\left\|\boldsymbol{r}_e-\boldsymbol{r}_i\right\|}-\frac{1}{c}\frac{x_e-x_j}{\left\|\boldsymbol{r}_e-\boldsymbol{r}_j\right\|}, \tag{3.9}$$

$$\frac{\partial\tau_{ij}}{\partial y_e}=\frac{1}{c}\frac{y_e-y_i}{\left\|\boldsymbol{r}_e-\boldsymbol{r}_i\right\|}-\frac{1}{c}\frac{y_e-y_j}{\left\|\boldsymbol{r}_e-\boldsymbol{r}_j\right\|}, \tag{3.10}$$

and

$$\frac{\partial\tau_{ij}}{\partial z_e}=\frac{1}{c}\frac{z_e-z_i}{\left\|\boldsymbol{r}_e-\boldsymbol{r}_i\right\|}-\frac{1}{c}\frac{z_e-z_j}{\left\|\boldsymbol{r}_e-\boldsymbol{r}_j\right\|}, \tag{3.11}$$

which can be written as

$$\frac{\partial \tau_{ij}}{\partial w_e} = \frac{1}{c}\frac{w_e - w_i}{\left\| \boldsymbol{r}_e - \boldsymbol{r}_i \right\|} - \frac{1}{c}\frac{w_e - w_j}{\left\| \boldsymbol{r}_e - \boldsymbol{r}_j \right\|}, \quad w \in \{x, y, z\}. \tag{3.12}$$

Equations (3.8) and (3.12) can be redefined with the matrix equation

$$Av = u \tag{3.13}$$

where A, v and u are defined as

$$A = \begin{bmatrix} \frac{\partial \tau_{12}}{\partial x_e} & \frac{\partial \tau_{12}}{\partial y_e} & \frac{\partial \tau_{12}}{\partial z_e} \\ \vdots & \vdots & \vdots \\ \frac{\partial \tau_{n-1,n}}{\partial x_e} & \frac{\partial \tau_{n-1,n}}{\partial y_e} & \frac{\partial \tau_{n-1,n}}{\partial z_e} \end{bmatrix}, \tag{3.14}$$

$$v = \begin{bmatrix} \Delta x_e \\ \Delta y_e \\ \Delta z_e \end{bmatrix}, \tag{3.15}$$

and

$$u = \begin{bmatrix} \Delta \tau_{ij} \\ \vdots \\ \Delta \tau_{n-1,n} \end{bmatrix}. \tag{3.16}$$

3. Linear Least-Squares Solution

The linear least-squares solution of (3.13) is the emitter-position error vector v. Since the matrix A has dimensions $n(n\text{-}1)/2$ by 3, which is not a square matrix, the pseudo inverse of A is used. The emitter-position error vector is obtained as

$$v = (A^T A)^{-1} A^T u. \tag{3.17}$$

The root-mean-squared (RMS) emitter-position error is

$$\|v\| = \sqrt{(\Delta x_e)^2 + (\Delta y_e)^2 + (\Delta z_e)^2}. \tag{3.18}$$

4. Three-Sensor System

a. Altitude Error

A three-satellite system to detect user-coordinate errors (Δx_u, Δy_u, Δz_u) is discussed in [9]. This is similar to the present problem of determining the emitter-position error (Δx_e, Δy_e, Δz_e) in a three-sensor system; hence, the mathematical model in [9] is adopted.

In [9], for the three-satellite system, four non-linear equations were used to determine the user coordinates (x_u, y_u, z_u) and user-coordinates error (Δx_u, Δy_u, Δz_u). The first three equations are derived from the differential-distance between two satellites, which is similar to (3.6). The fourth equation utilized the user altitude h_u and can also be used with the emitter altitude h_e as

$$x_e^{\,2} + y_e^{\,2} + z_e^{\,2} = (R + h_e)^2, \tag{3.19}$$

where R is the earth radius. Equation (3.19) can be rewritten as

$$h_e = \sqrt{\left(x_e^{\,2} + y_e^{\,2} + z_e^{\,2}\right)} - R. \tag{3.20}$$

The partial differentiation of (3.20) with respect to x, y, and z gives the altitude error

$$\Delta h_e = \frac{\partial h_e}{\partial x_e}\Delta x_e + \frac{\partial h_e}{\partial y_e}\Delta y_e + \frac{\partial h_e}{\partial z_e}\Delta z_e, \tag{3.21}$$

and the partial derivatives are

$$\frac{\partial h_e}{\partial x_e} = \frac{x_e}{\sqrt{x_e^{\,2} + y_e^{\,2} + z_e^{\,2}}}, \tag{3.22}$$

$$\frac{\partial h_e}{\partial y_e} = \frac{y_e}{\sqrt{x_e^{\,2} + y_e^{\,2} + z_e^{\,2}}}, \tag{3.23}$$

and

$$\frac{\partial h_e}{\partial z_e} = \frac{z_e}{\sqrt{x_e^{\,2} + y_e^{\,2} + z_e^{\,2}}}. \tag{3.24}$$

Now (3.21) can be written as the emitter-altitude error

$$\Delta h_e = \frac{x_e(\Delta x_e) + y_e(\Delta y_e) + z_e(\Delta z_e)}{\sqrt{x_e{}^2 + y_e{}^2 + z_e{}^2}} = \frac{x_e(\Delta x_e) + y_e(\Delta y_e) + z_e(\Delta z_e)}{R + h_e}. \tag{3.25}$$

Equation (3.25) together with (3.14) and (3.17) can be formed into another linear least square equation

$$Bv = m, \tag{3.26}$$

where *B*, *v* and *m* are defined, respectively,

$$B = \begin{bmatrix} \frac{\partial \tau_{12}}{\partial x_e} & \frac{\partial \tau_{12}}{\partial y_e} & \frac{\partial \tau_{12}}{\partial z_e} \\ \frac{\partial \tau_{13}}{\partial x_e} & \frac{\partial \tau_{13}}{\partial y_e} & \frac{\partial \tau_{13}}{\partial z_e} \\ \frac{\partial \tau_{23}}{\partial x_e} & \frac{\partial \tau_{23}}{\partial y_e} & \frac{\partial \tau_{23}}{\partial z_e} \\ \frac{x_e}{R + h_e} & \frac{y_e}{R + h_e} & \frac{z_e}{R + h_e} \end{bmatrix}, \tag{3.27}$$

$$v = \begin{bmatrix} \Delta x_e \\ \Delta y_e \\ \Delta z_e \end{bmatrix}, \tag{3.28}$$

and

$$m = \begin{bmatrix} \Delta \tau_{12} \\ \Delta \tau_{13} \\ \Delta \tau_{23} \\ \Delta h_e \end{bmatrix}. \tag{3.29}$$

b. Modified Linear Least-Squares Solution

Similar to reference [9], the error contribution in the *z*-coordinate in (3.8) and (3.25) is observed to be much less than the error contribution in the *x*- and *y*-coordinates; hence, the modified linear least-squares solution from [9] is adopted for the error analysis model.

The modified least-squares approach aimed to obtain a more accurate estimate of Δz. The least-squares estimate of Δx and Δy is first derived without the contribution of Δz. Subsequently, Δz is obtained using Δx and Δy. The emitter-position error vector v in (3.28) is obtained from (3.26) with modifications to matrix B and v, where

$$v = \begin{bmatrix} v_1 \\ \Delta z_e \end{bmatrix}, \tag{3.30}$$

$$v_1 = \begin{bmatrix} \Delta x_e \\ \Delta y_e \end{bmatrix} = (B_1^T B_1)^{-1} B_1^T m, \tag{3.31}$$

$$\Delta z_e = (B_2^T B_2)^{-1} (B_2^T m - B_2^T B_1 v_1), \tag{3.32}$$

$$B_1 = \begin{bmatrix} \dfrac{\partial \tau_{12}}{\partial x_e} & \dfrac{\partial \tau_{12}}{\partial y_e} \\ \dfrac{\partial \tau_{13}}{\partial x_e} & \dfrac{\partial \tau_{13}}{\partial y_e} \\ \dfrac{\partial \tau_{23}}{\partial x_e} & \dfrac{\partial \tau_{23}}{\partial y_e} \\ \dfrac{x_e}{R + h_e} & \dfrac{y_e}{R + h_e} \end{bmatrix}, \tag{3.33}$$

and

$$B_2 = \begin{bmatrix} \dfrac{\partial \tau_{12}}{\partial z_e} \\ \dfrac{\partial \tau_{13}}{\partial z_e} \\ \dfrac{\partial \tau_{23}}{\partial z_e} \\ \dfrac{z_e}{R + h_e} \end{bmatrix}. \tag{3.34}$$

5. Four-Sensor System

In the four-sensor system, the modified least-squares solution is used. The emitter-position error vector *v* is obtained from Equations (3.30) to (3.32) and (3.35) to (3.36), where

$$B_1 = \begin{bmatrix} \frac{\partial \tau_{12}}{\partial x_e} & \frac{\partial \tau_{12}}{\partial y_e} \\ \frac{\partial \tau_{13}}{\partial x_e} & \frac{\partial \tau_{13}}{\partial y_e} \\ \frac{\partial \tau_{14}}{\partial x_e} & \frac{\partial \tau_{14}}{\partial y_e} \\ \frac{x_e}{R+h_e} & \frac{y_e}{R+h_e} \end{bmatrix} \tag{3.35}$$

and

$$B_2 = \begin{bmatrix} \frac{\partial \tau_{12}}{\partial z_e} \\ \frac{\partial \tau_{13}}{\partial z_e} \\ \frac{\partial \tau_{14}}{\partial z_e} \\ \frac{z_e}{R+h_e} \end{bmatrix}. \tag{3.36}$$

To obtain the matrix in (3.35) for the four-sensor system, partial derivatives of τ_{23} with respect to x_e and y_e in (3.33) are replaced with partial derivatives of τ_{14}. As for (3.36), the partial derivative of τ_{23} with respect to z_e in (3.34) is replaced with the partial derivative of τ_{14}.

D. TEST CASES FOR THREE-SENSOR SYSTEM

The test cases were created to determine how the input variables affect the localization error of the emitter. The results are observed and discussed in Chapter IV.

1. Effect of Primary Variables

Test cases 1 and 2 aim to provide an insight into how the primary variables affect the localization error of the emitter.

a. Test Case 1: Worst Case of RMS Emitter-Position Error

The purpose of this case is to derive the extreme case of the RMS emitter-position error by finding the worst case of the primary input variables. The primary variables are the TDOA error and sensor-position error.

The TDOA error $\Delta\tau_{ij}$ is proportional to the differential-distance error $c\Delta\tau_{ij}$. To provide a comparison to sensor-position error in the same units of measurement, the sensor differential-distance error is used instead of TDOA error from here on.

In a three-sensor system, the altitude error Δh_e in (3.29) has the same error limits as the sensor-position error since they are both position errors.

The variables for test case 1 are in Table 2, where $w \in \{x, y, z\}$. The ranges of values of input variables are stated for each test case. Test case 1a has the lowest range limits, while test case 1b has the highest range limits. It is expected that the results of test case 1a will provide the lowest emitter-position error, and the opposite is expected from test case 1b. Test case 1c aims to provide insight to the effect of sensor-position error and emitter-altitude error. The differences between test case 1a and 1c are the limits for sensor-position error and emitter-altitude error.

Table 2. Discrete variables for worst case of RMS emitter-position error.

	Discrete variables		
Test case no.	**Sensor differential-distance error**	**Sensor-position error**	**Emitter-altitude error**
1a	10 m $\le \lvert c\Delta\tau_{ij}\rvert \le$ 20 m, increments of 1 m	0.2 m $\le \lvert\Delta w_i\rvert \le$ 2 m, increments of 0.1 m	0.2 m $\le \lvert\Delta h_e\rvert \le$ 2 m, increments of 0.1 m
1b	20 m $\le \lvert c\Delta\tau_{ij}\rvert \le$ 40 m, increments of 2 m	1 m $\le \lvert\Delta w_i\rvert \le$ 4 m, increments of 0.2 m	1 m $\le \lvert\Delta h_e\rvert \le$ 4 m, increments of 0.2 m
1c	10 m $\le \lvert c\Delta\tau_{ij}\rvert \le$ 20 m, increments of 1 m	1 m $\le \lvert\Delta w_i\rvert \le$ 4 m, increments of 0.2 m	1 m $\le \lvert\Delta h_e\rvert \le$ 4 m, increments of 0.2 m

b. Test Case 2: Uniform Random Distribution

The primary variables, the sensor differential-distance error and sensor-position error, were chosen to be uniform random variables. In a three-sensor system, the altitude error Δh_e in (3.29) has the same error limits as the sensor-position error since they are both position errors. The input variables for test cases 2a to 2c are the same for test cases 1a to 1c.

Table 3. Uniform random variables for RMS emitter-position error (test cases 2a to 2c).

	Uniform random variables		
Test case no.	**Sensor differential-distance error**	**Sensor-position error**	**Emitter-altitude error**
2a	$10\text{ m} \le \lvert c\Delta\tau_{ij}\rvert \le 20\text{ m}$	$0.2\text{ m} \le \lvert\Delta w_i\rvert \le 2\text{ m}$	$0.2\text{ m} \le \lvert\Delta h_e\rvert \le 2\text{ m}$
2b	$20\text{ m} \le \lvert c\Delta\tau_{ij}\rvert \le 40\text{ m}$	$1\text{ m} \le \lvert\Delta w_i\rvert \le 4\text{ m}$	$1\text{ m} \le \lvert\Delta h_e\rvert \le 4\text{ m}$
2c	$10\text{ m} \le \lvert c\Delta\tau_{ij}\rvert \le 20\text{ m}$	$1\text{ m} \le \lvert\Delta w_i\rvert \le 4\text{ m}$	$1\text{ m} \le \lvert\Delta h_e\rvert \le 4\text{ m}$

2. Effect of Secondary Variables

To study the effects of secondary variables on the localization error of the emitter, the primary variables were chosen as random variables with a uniform distribution. The limits of the primary variables are described in Table 4.

Table 4. Uniform random variables for RMS emitter-position error (test cases 3a to 3c).

	Uniform random variables		
Test case no.	**Sensor differential-distance error**	**Sensor-position error**	**Emitter-altitude error**
3a	$10\text{ m} \le \lvert c\Delta\tau_{ij}\rvert \le 20\text{ m}$	$0.2\text{ m} \le \lvert\Delta w_i\rvert \le 2\text{ m}$	$0.2\text{ m} \le \lvert\Delta h_e\rvert \le 2\text{ m}$
3b	$20\text{ m} \le \lvert c\Delta\tau_{ij}\rvert \le 40\text{ m}$	$1\text{ m} \le \lvert\Delta w_i\rvert \le 4\text{ m}$	$1\text{ m} \le \lvert\Delta h_e\rvert \le 4\text{ m}$
3c	$10\text{ m} \le \lvert c\Delta\tau_{ij}\rvert \le 20\text{ m}$	$1\text{ m} \le \lvert\Delta w_i\rvert \le 4\text{ m}$	$1\text{ m} \le \lvert\Delta h_e\rvert \le 4\text{ m}$

In addition to the primary variables in each test case, the secondary variables are:

a) altitude of sensors,
b) distance between emitter and sensors, and
c) number of sensors (three or four).

a. Altitude of Sensors

In order to study the effects of sensor altitude on the RMS emitter-position error, the uniformly distributed random primary variables in test cases 2a to 2c were used.

The sensor altitude is selected based on three criteria:

- low altitude ($0 \text{ m} \leq h_i \leq 100 \text{ m}$),
- high altitude ($100 \text{ m} < h_i \leq 300 \text{ m}$), and
- random altitude ($0 \text{ m} \leq h_i \leq 300 \text{ m}$).

b. Range Between Emitter and Sensors

The range between emitter and sensors can affect the localization error. The maximum range between emitter and sensor was varied so that the effects could be observed.

The maximum ranges, 1 km, 3 km, 5 km, 10 km, 15 km, and 20 km, were chosen as test values. For larger ranges such as 5 km and greater, the line-of-sight communications is limited at lower altitude; hence, the altitude of the sensors was chosen to be higher. The maximum ranges and sensor altitudes in Table 5 were used together with test cases 3a to 3b.

Table 5. Maximum range and sensor altitude.

Maximum range (km)	**Sensor altitude (m)**
1	0-300
3	0-300
5	300-600
10	300-1500
15	300-1500
20	300-2000

E. TEST CASES FOR FOUR-SENSOR SYSTEM

It is intuitive that increasing the number of sensors causes the localization error to decrease. The scenario with four sensors was tested, and the primary variables were the

same as for the three-sensor system. The primary variables and their values are stated for test cases 4a to 4c in Table 6. The results from both the three-sensor system and four-sensor system are analyzed in Chapter IV.

Table 6. Discrete variables for worst case of RMS emitter-position error (four sensors).

	Discrete variables		
Test case no.	**Sensor differential-distance error**	**Sensor-position error**	**Emitter-altitude error**
4a	10 m $\leq \lvert c\Delta\tau_{ij}\rvert \leq$ 20 m, increments of 1 m	0.2 m $\leq \lvert\Delta w_i\rvert \leq$ 2 m, increments of 0.1 m	0.2 m $\leq \lvert\Delta h_e\rvert \leq$ 2 m, increments of 0.1 m
4b	20 m $\leq \lvert c\Delta\tau_{ij}\rvert \leq$ 40 m, increments of 2 m	1 m $\leq \lvert\Delta w_i\rvert \leq$ 4 m, increments of 0.2 m	1 m $\leq \lvert\Delta h_e\rvert \leq$ 4 m, increments of 0.2 m
4c	10 m $\leq \lvert c\Delta\tau_{ij}\rvert \leq$ 20 m, increments of 1 m	1 m $\leq \lvert\Delta w_i\rvert \leq$ 4 m, increments of 0.2 m	1 m $\leq \lvert\Delta h_e\rvert \leq$ 4 m, increments of 0.2 m

F. SOFTWARE SIMULATION

The software simulation for test cases 1 to 4 is described in this section. The software used was Matlab. Test cases 1 and 4 use discrete variables to find the worst case of emitter-position error, while test cases 2 and 3 use variables with a uniform distribution to generate statistics of the emitter-position error.

For each test case, the main variables and ranges of variables are the same. The main variables are sensor differential-distance error, sensor-position error and emitter-altitude error. The main differences in the test case are the distribution and values used for the simulation.

1. Terms Used In The Simulation

- Test Sample

A test sample is a scenario consisting of one emitter and n sensors, where n = 3 or 4. This test sample was evaluated based on the mathematical model and the input variables for the test case. For the test sample, the location of the emitter and sensor positions were provided in GPS coordinates.

- Sensor Group

A sensor group is a set of sensors which have positions randomly selected for the experiment. The sensor groups are labeled A1 to A4 and B1 to B4. The Matlab code was written such that it can efficiently calculate a large number of test samples in one run. A typical number of test samples is 500, where 500 emitter positions were evaluated with the same sensor group.

2. Worst Case of Emitter-Position Error

a. Test Procedure

The test procedure was written for one test sample in the three-sensor system but is similar for the four-sensor system.

i. For one test sample, the sensor differential-distance error $c\Delta\tau_{ij}$ was chosen from the first value within the range, such as 10 m.
ii. The sensor-position error Δw_i and emitter-altitude error Δh_e were also chosen from the first value within the range, such as 0.2 m.
iii. The error vector m in Equation (3.29) was created using the values obtained in (ii). Each Δw_i takes on the positive error value such as 0.2 m or negative error value such as -0.2 m. As there are four components in vector m, the total number of possible combinations for vector m is 16.
iv. The 16 combinations of m were iterated, and the emitter-position error was evaluated for each combination. The RMS of the error was taken and the largest RMS error was saved for reference later.
v. The steps (ii) to (iv) were repeated for the next value of sensor-position error Δw_i and emitter-altitude error Δh_e. At the end of this step, the largest RMS error for one value of $c\Delta\tau_{ij}$ is obtained.
vi. The steps (i) to (v) were repeated for all other discrete values of $c\Delta\tau_{ij}$.

b. Tabulation of Results

At the end of evaluation of one test sample, there was a largest RMS error for each Δw_i and $c\Delta\tau_{ij}$. The typical number of test samples used was 500. The largest RMS error for each Δw_i was averaged among the 500 test samples. The same averaging method was performed for $c\Delta\tau_{ij}$. The graphs of RMS errors were then plotted against Δw_i and $c\Delta\tau_{ij}$.

3. Mean Emitter-Position Error

a. Test Procedure

i. For one test sample, the sensor differential-distance error $c\Delta\tau_{ij}$ is a random variable from a uniform distribution within a specified range. The $c\Delta\tau_{ij}$ was randomly selected.
ii. The sensor-position error Δw_i and emitter-altitude error Δh_e were chosen as random variables from a uniform distribution.
iii. The error vector m in Equation (3.29) was created using the values obtained in (ii).
iv. The emitter-position error was evaluated and the RMS error was recorded.

b. Tabulation of Results

At the end of evaluation of one test sample, there was one RMS error for each emitter. The RMS error was averaged among all 500 test samples. The standard deviation was also evaluated from all the test samples.

THIS PAGE INTENTIONALLY LEFT BLANK

IV. NUMERICAL RESULTS

The numerical results obtained from the modeling and simulation approach in Chapter III is presented here.

A. RESULTS FOR THREE-SENSOR SYSTEM

The results for three-sensor system are analyzed in this section.

1. Trends Due to Primary Variables

The primary variables are the differential-distance error and the sensor-position error. Their effects on the RMS emitter-position error are presented, and the results for both test cases 1a to 1c and 2a to 2c are compared.

a. Observations in Test Cases 1A To 1C

The observations of the effects of differential-distance error and sensor-position error are separately discussed in the following sections.

(1) RMS emitter-position error $\|v\|$ vs differential-distance error $c\Delta\tau_{ij}$

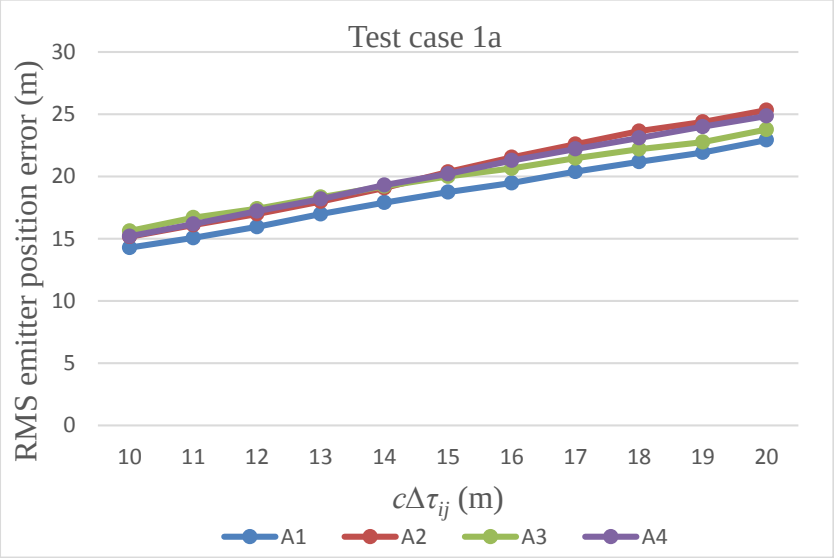

Figure 1. RMS emitter-position error $\|v\|$ vs differential-distance error $c\Delta\tau_{ij}$ (Test case 1a).

The RMS emitter-position error $\|v\|$ increases as the differential-distance error $c\Delta\tau_{ij}$ increases. This is consistent for all test cases 1a to 1c, as shown in Figures 1 to 3. The sensor groups A1 to A4 have positions, which are randomly selected, and they gave rise to similar results in each test case.

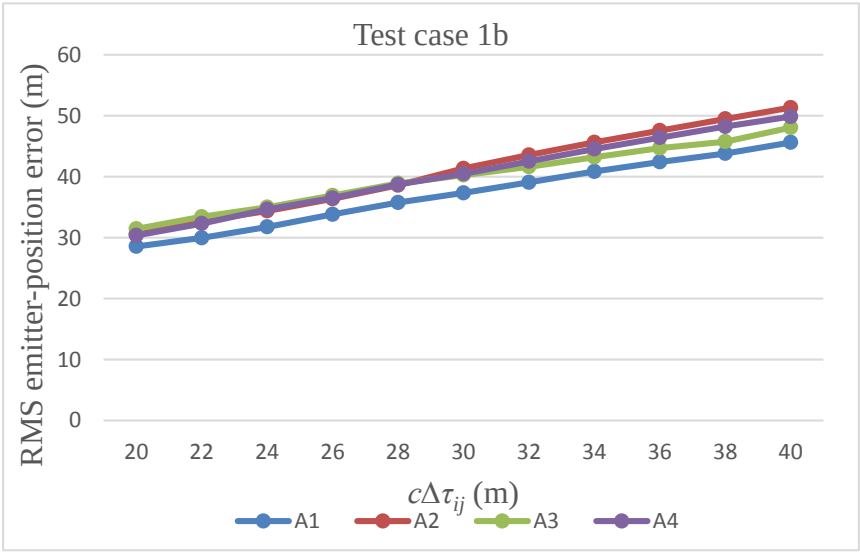

Figure 2. RMS emitter-position error $\|v\|$ vs differential-distance error $c\Delta\tau_{ij}$ (Test case 1b).

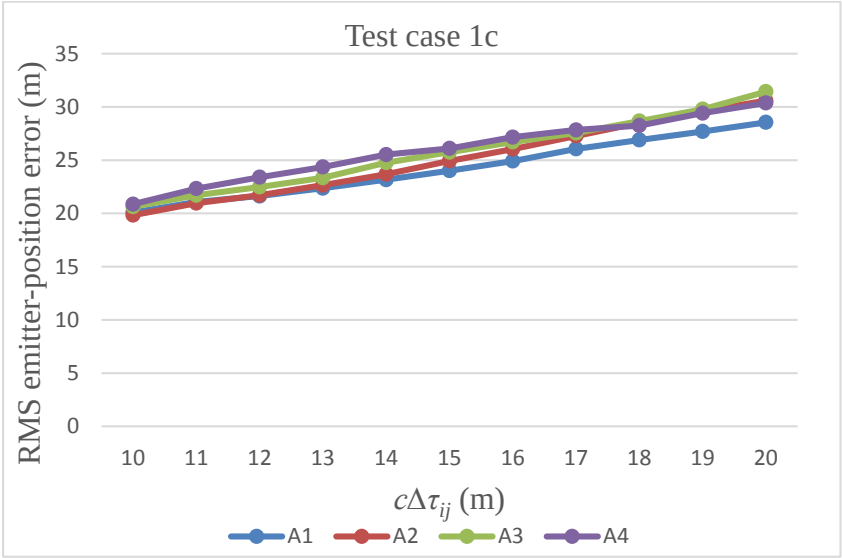

Figure 3. RMS emitter-position error $\|v\|$ vs differential-distance error $c\Delta\tau_{ij}$ (Test case 1c).

(2) RMS emitter-position error $\|v\|$ vs sensor-position error Δw_i

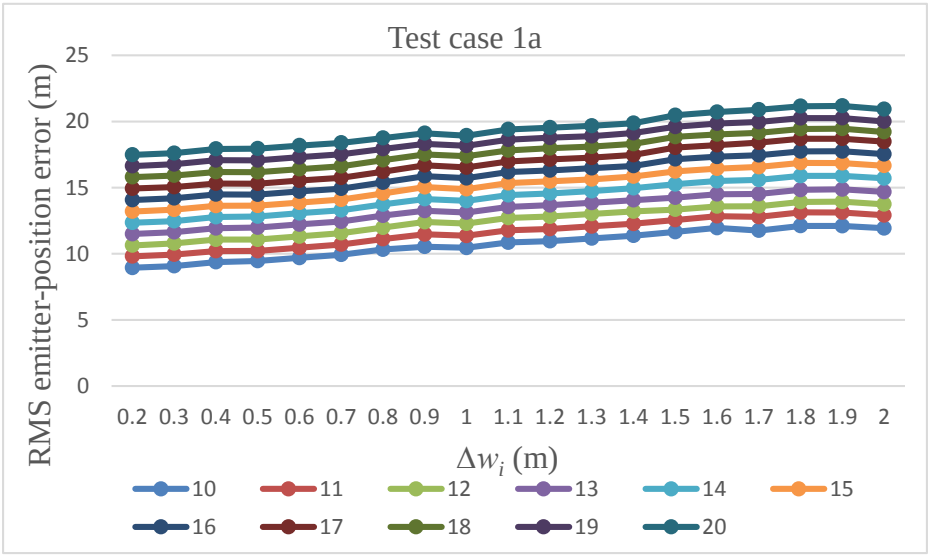

Figure 4. RMS emitter-position error $\|v\|$ vs sensor-position error Δw_i (Test case 1a).

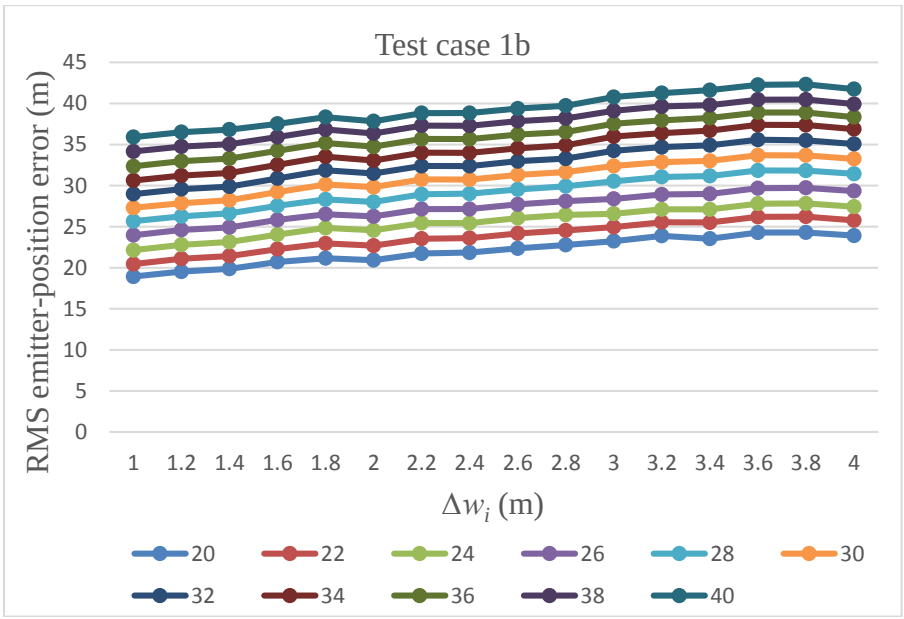

Figure 5. RMS emitter-position error $\|v\|$ vs sensor-position error Δw_i (Test case 1b).

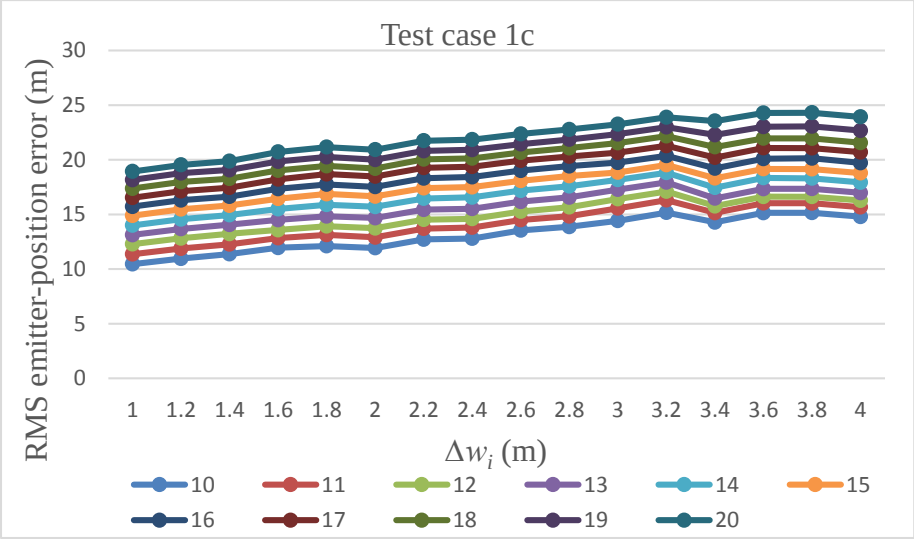

Figure 6. RMS emitter-position error $\|v\|$ vs sensor-position error Δw_i (Test case 1c).

For this analysis, the differential-distance errors $c\Delta\tau_{ij}$ were taken at discrete values from 10 m to 20 m or from 20 m to 40 m. For a fixed differential-distance error, the sensor-position error was taken at discrete values from 0.2 m to 2 m or from 1 m to 4 m. It is observed that when the sensor-position error Δw_i increases, the RMS position error for emitter $\|v\|$ increases. This is consistent for all test cases 1a to 1c, as shown in Figures 4 to 6. For test case 1c, as shown in Figure 6, there was an unexpected small decrease in the RMS emitter-position error for differential-distance error $c\Delta\tau_{ij}$ greater than 3.2 m. It is observed that there was a larger decrease for differential-distance error at 10 m as compared to 20 m. This is likely because sensor-position errors which are greater than 3.2 m form a larger percentage of differential-distance at 10 m as compared to 20 m.

b. Observations in Test Cases 2A To 2C

In test cases 2a to 2c, the sensor-position error and differential-distance error were modeled as uniform random variables. With a larger differential-distance error $c\Delta\tau_{ij}$, the RMS emitter-position error and standard deviation were relatively larger, as shown in Table 7. Results from test cases 2a and 2b provide the lowest and highest mean of emitter-position error, respectively. Test case 2c is indicative in that sensor-position

errors of less than 4.0 m contribute to a 32.7% increase in mean emitter-position error as compared to test case 2a.

Table 7. Emitter-position error for test cases 2a to 2c.

Test case no.	Sensor-position error	Differential-distance error	Emitter-position error	
			Mean (m)	Standard deviation (m)
2a	0.2 m<$\|\Delta w_i\|$<2 m	10 m<$\|c\Delta\tau_{ij}\|$<20 m	8.062	7.863
2b	1 m<$\|\Delta w_i\|$<4 m	20 m<$\|c\Delta\tau_{ij}\|$<40 m	17.1795	16.210
2c	1 m<$\|\Delta w_i\|$<4 m	10 m<$\|c\Delta\tau_{ij}\|$<20 m	10.699	8.311

c. Comparison of Test Cases 1A To 1C and 2A To 2C

For all test cases, the mean and standard deviation increased when the differential-distance error $c\Delta\tau_{ij}$ and sensor-position error Δw_i increased. The results of test cases 1a to 1c were verified to be the worst case since they are larger than the results of test cases 2a to 2c, where uniformly distributed random variables were used.

Table 8. Emitter-position error statistics for test cases 1a to 1c and 2a to 2c.

Test case no.	Sensor-position error	Differential-distance error	Emitter-position error	
			Mean (m)	Standard deviation (m)
1a	0.2 m<$\|\Delta w_i\|$<2 m	10 m<$\|c\Delta\tau_{ij}\|$<20 m	19.734	12.149
2a			8.062	7.863
1b	1 m<$\|\Delta w_i\|$<4 m	20 m<$\|c\Delta\tau_{ij}\|$<40 m	39.652	24.339
2b			17.1795	16.210
1c	1 m<$\|\Delta w_i\|$<4 m	10 m<$\|c\Delta\tau_{ij}\|$<20 m	25.229	15.139
2c			10.699	8.311

2. Trends Due To Secondary Variables

a. Sensor Altitude

Test cases 3a to 3c were carried out with the emitter-altitude ranges from 0 to 300 m. It is observed from Table 9 that both larger and random sensor altitudes yielded smaller RMS emitter-position errors than sensors at lower altitudes. It is likely that at lower altitudes, the distance between emitter and sensors are smaller; hence, any error

was greater, resulting in larger RMS emitter-position errors. It is to be noted that sensors at random altitudes can achieve localization errors that are as small as that of sensors at high altitude.

Table 9. Emitter-position error vs sensor altitude.

Test case no.	Emitter-position error					
	Sensors at low altitude (0 m ≤ h_i ≤100 m)		Sensors at high altitude (100 m < h_i ≤ 300 m)		Sensors at random altitude (0 m ≤ h_i ≤ 300 m)	
	Mean (m)	Standard deviation (m)	Mean (m)	Standard deviation (m)	Mean (m)	Standard deviation (m)
3a	8.216	8.169	7.666	7.312	7.678	7.550
3b	17.444	16.813	16.367	15.388	15.819	14.713
3c	10.477	8.399	9.940	8.355	9.905	7.673

Table 10. Emitter-position error derived from various maximum ranges.

Test case no.	Maximum range	Sensor altitude	Emitter-position error	
			Mean (m)	Standard deviation (m)
3a	1 km	0-300 m	7.678	7.550
	3 km	0-300 m	7.879	7.157
	5 km	300-600 m	9.541	8.669
	10 km	300-1500 m	9.400	8.001
	15 km	300-1500 m	9.244	7.581
	20 km	300-2000 m	9.927	9.104
3b	1 km	0-300 m	15.819	14.713
	3 km	0-300 m	15.974	13.283
	5 km	300-600 m	19.791	17.950
	10 km	300-1500 m	18.148	15.895
	15 km	300-1500 m	19.243	15.333
	20 km	300-2000 m	19.875	17.065
3c	1 km	0-300 m	9.905	7.673
	3 km	0-300 m	10.383	7.507
	5 km	300-600 m	11.977	9.531
	10 km	300-1500 m	12.106	8.598
	15 km	300-1500 m	12.654	9.279
	20 km	300-2000 m	12.467	9.530

b. Range Between Emitter and Sensors

The position error results for various values of maximum ranges and sensor altitudes are presented in Table 10. It is observed that as the maximum range increases, the mean error increases; however, for maximum ranges at 10 km and larger, the error was very similar for each test case. It seems that the error converges to a maximum after 10 km. The gain in sensor altitude does not necessarily improve the emitter-position error for larger maximum ranges.

B. SIMULATION RESULTS FOR FOUR-SENSOR SYSTEM

The following results are for the four-sensor system. They are compared to the test cases 1a to 1c for the three-sensor system.

1. Observations In Test Cases 4A To 4C

The results for the test cases are presented below. Similar to the three-sensor system, the emitter-position error from the four-sensor system is almost linearly proportional to the sensor differential-distance error (or TDOA error) and the sensor-position error.

(1) RMS emitter-position error $\|v\|$ vs differential-distance error $c\Delta\tau_{ij}$

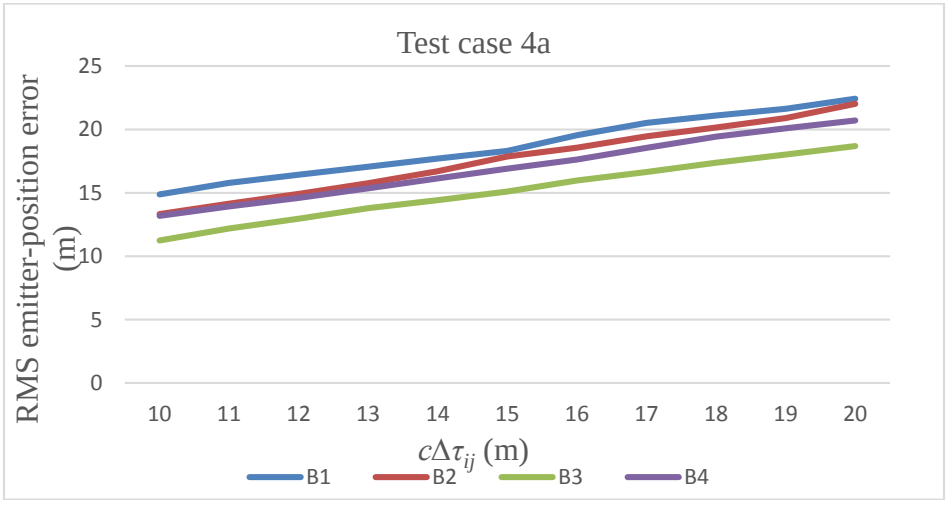

Figure 7. RMS emitter-position error $\|v\|$ vs differential-distance error $c\Delta\tau_{ij}$ (Test case 4a).

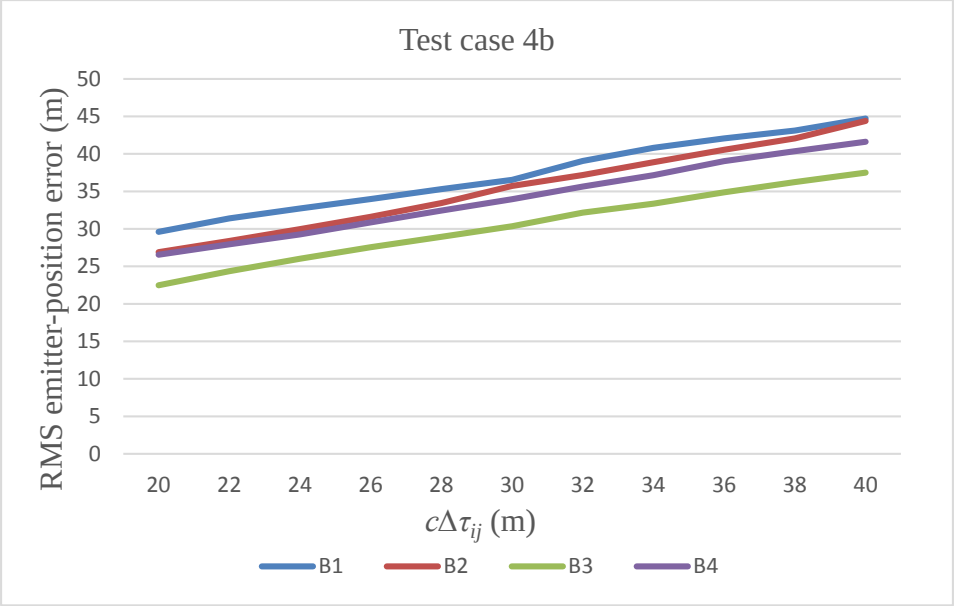

Figure 8. RMS emitter-position error $\|v\|$ vs differential-distance error $c\Delta\tau_{ij}$ (Test case 4b).

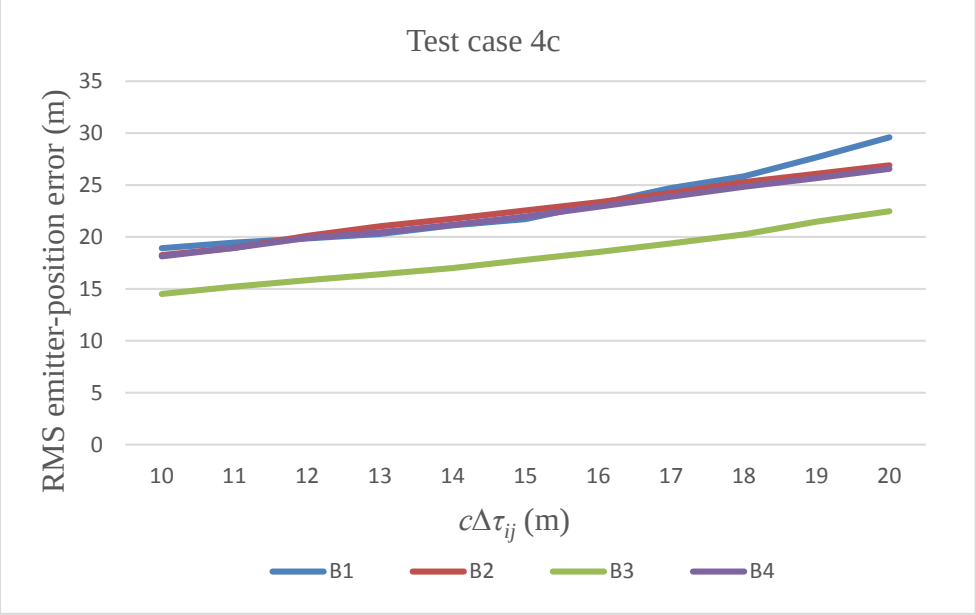

Figure 9. RMS emitter-position error $\|v\|$ vs differential-distance error $c\Delta\tau_{ij}$ (Test case 4c).

As the differential-distance error $c\Delta\tau_{ij}$ increases, the RMS emitter-position error $\|v\|$ increases. This is consistent for all test cases 4a to 4c, as shown in Figures 7 to 9. The

sensor groups B1 to B4 have positions which were randomly selected, and they give rise to similar results for each test case.

(2) RMS emitter-position error $\|v\|$ vs sensor-position error Δw_i

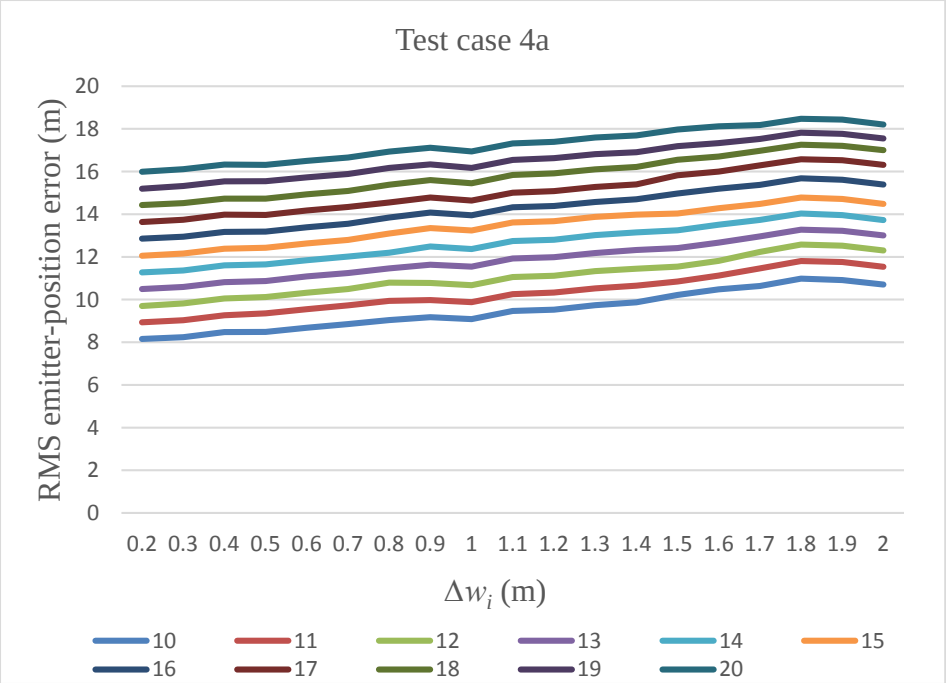

Figure 10. RMS emitter-position error $\|v\|$ vs sensor-position error Δw_i (Test case 4a).

Given a specific differential-distance error ($c\Delta\tau_{ij}$ = 10, 11, … 20 or $c\Delta\tau_{ij}$ = 20, 22, … 40), when the sensor-position error Δw_i increased, the RMS position error of emitter $\|v\|$ generally increased. This was consistent for all test cases 4a to 4c, as shown in Figures 10 to 12. Test case 4c, as shown in Figure 12, had an unexpected small decrease in the RMS emitter-position error for differential-distance errors $c\Delta\tau_{ij}$ greater than 3.2 m. This is likely due to the sensor-position errors larger than 3.2 m contributing to a large percentage of the differential-distance errors; hence, the decrease in RMS emitter-position error is larger for a differential-distance of 10.0 m than for 20.0 m.

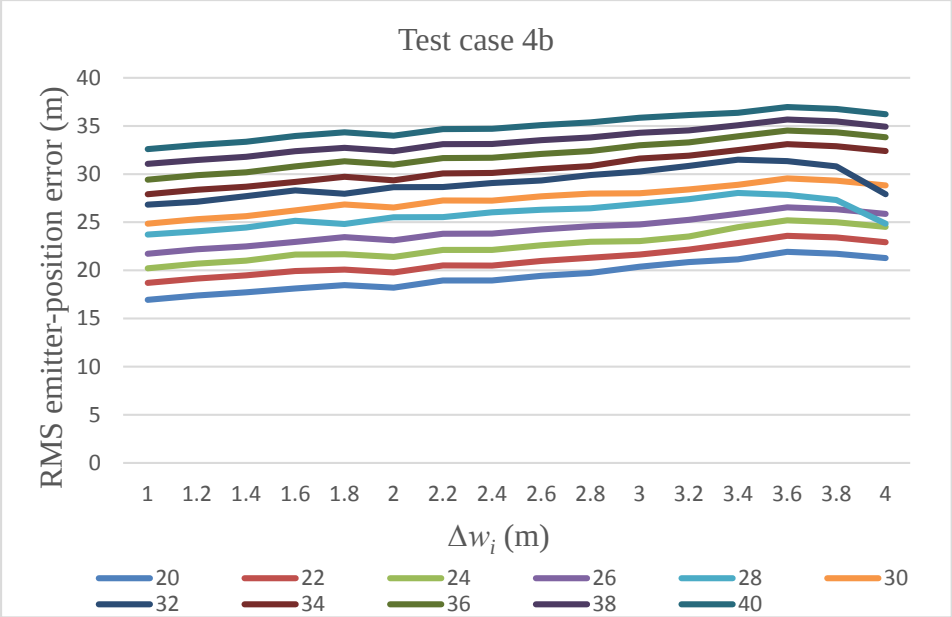

Figure 11. RMS emitter-position error $\|v\|$ vs sensor-position error Δw_i (Test case 4b).

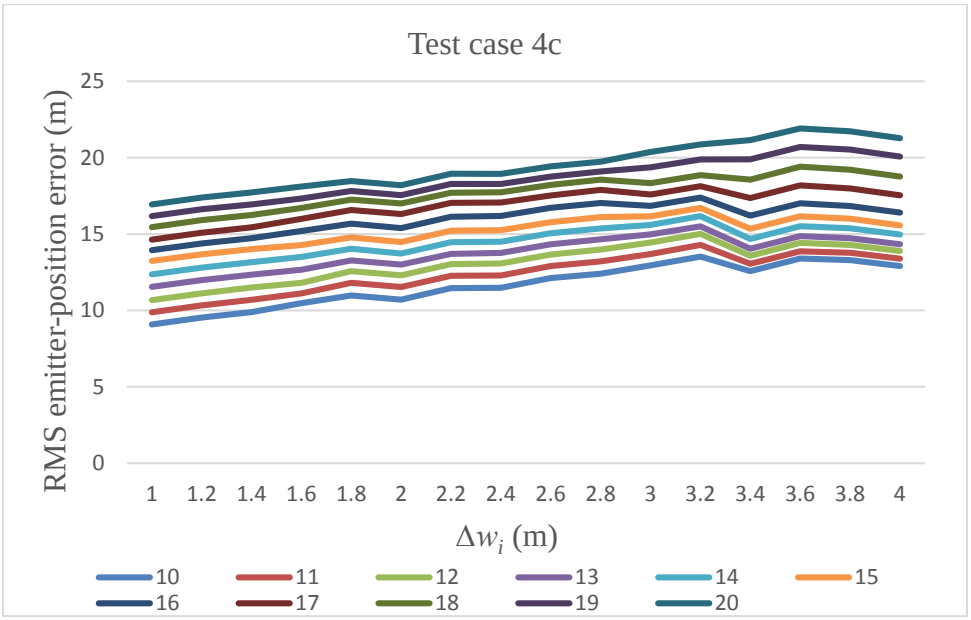

Figure 12. RMS emitter-position error $\|v\|$ vs sensor-position error Δw_i (Test case 4c).

2. Comparison of Test Cases 1A To 1C and 4A To 4C

The test cases 1a to 1c were for the three-sensor system, while test cases 4a to 4c were for the four-sensor system. The results for the three-sensor system, as shown in Table 11, was satisfactory as the mean emitter-position error is near the upper limit of the differential-distance error for each test case. In test case 1a, the upper limit of differential-distance error is 20.0 m, and the mean emitter-position error is 19.734 m. This is also true for test case 1b. For test case 1c, the mean emitter-position error of 25.229 m is greater than the upper limit of differential-distance of 20.0 m. This is likely due to the sensor-position error. The upper limit of sensor-position error was 4.0 m and constitutes 20% of the differential-distance position error.

The emitter-position errors are smaller for the four-sensor system, as shown in Table 11. This is evidence that the four-sensor system performs better than the three-sensor system, in this case, by more than 13%.

Table 11. Emitter-position error statistics for test cases 1a to 1c and 4a to 4c.

	Emitter-position error		
Test case no.	**Mean (m)**	**Decrease in the mean (%)**	**Standard deviation (m)**
1a	19.734	13.55	12.149
4a	17.058		10.370
1b	39.652	13.80	24.339
4b	34.178		20.517
1c	25.229	15.38	15.139
4c	21.660		12.660

C. OTHER OBSERVATIONS

In addition to the effects resulting from the primary and secondary variables, there are other observations during the Matlab modeling and simulation phase.

1. Comparison of Two Solution Methods

As explained in the mathematical model, the modified least-squares solution is used to give a better estimate of the errors in *x*-, *y*-, and *z*-coordinates. To illustrate the

explanation, the two solution methods were given the same input variables, and the results are presented in Table 14.

Table 12. Comparison of localization error from two solution methods.

Localization error	Least-squares method (m)	Modified least-squares method (m)
Δx	-32.0	8.0
Δy	1248.0	-16.0
Δz	0	10.8

The least-squares method results in a poor estimation of the localization error; therefore, the modified least-squares method is used in our final model.

2. Error Is Larger Near The Equator

In [4], it was observed that error is larger when the user position is near the equator. This is due to the inherent characteristics of the geocentric Cartesian coordinate system. Although larger errors were observed for areas near the equator, as shown in Table 15, the errors are still acceptable.

Table 13. Emitter-position error vs latitude.

Test Case	Latitude	Emitter-position error mean (m)	Emitter-position error standard deviation (m)
2a	45˚N	7.678	7.550
	10˚N	8.121	7.244
	5˚N	10.811	9.020
2b	45˚N	15.819	14.713
	10˚N	17.081	14.130
	5˚N	22.666	18.038
2c	45˚N	9.905	7.673
	10˚N	12.623	9.364
	5˚N	18.214	15.724

D. RESULTS AND ANALYSIS

It is observed that, in the three-sensor system, the error position of the emitter increases almost linearly with the increase in sensor differential-distance errors (or TDOA error) and sensor-position errors. The worst case is test case 1b, where the differential-distance error was as large as +/-40 m, and the localization error was 39.652 m. This is evidence that the mathematical model is able to provide a localization error which is approximately equal to the differential-distance error.

The higher sensor altitude was predicted to provide a smaller error; however, this was not the case, as the random sensor altitude resulted in an error as small as that of the higher sensor altitude. The difference may not be evident in the numerical results; however, simulation for a highly urbanized environment could provide better insight into the effects of sensor altitude on the localization error of the emitter.

The localization error is directly proportional to the maximum range when the maximum range is 10 km or less. When the maximum range is greater than 10 km, the localization error does not get worse. This is due to the fact that sensors are placed at a higher altitude in order to get line-of-sight communications with the emitter.

The four-sensor system was proven to perform better than the three-sensor system. This may not be practical in localization applications as the resources may be limited. Nonetheless, four sensors are preferred.

The variable with the greatest effect on localization error was the TDOA error. The TDOA errors directly impact the emitter-position error due to the mathematical model used. The TDOA errors rely heavily on the accuracy of TDOA algorithms. Future work should include improvements to the algorithms mentioned in Chapter II.

The variable with the least effect was the altitude of the sensors. Although the altitude of sensors does not have a large impact on emitter-position error, we predict that sensor altitude may pose problems in practical applications in a highly urbanized environment.

This chapter concludes the TDOA error analysis, which forms part one of the thesis. In the next two chapters, the adaptive localization strategies are discussed.

V. REVIEW OF IEEE 802.22

IEEE 802.22 is the first standard to fully integrate the CR concept in the wireless network [2]; hence, it is used as a reference for the discussion of adaptive localization methods of CRs in Chapter VI. A summary and analysis of the CR capability in IEEE 802.22 cognitive radio network (CRN), in particular the SSF and spectrum-sensing technique and geolocation mechanism, is discussed in this chapter.

A. PURPOSE

IEEE 802.22 is the standard for wireless regional area networks (WRAN) which use the unused spectrum, or white spaces, in the television (TV) frequency spectrum [13]. The objective of IEEE 802.22 is to allow the sharing of unused TV spectrum within a geographical area by using CR methods so as not to cause interference [13] and aims to bring broadband access to rural and low population density areas [13].

The TV spectrum is desirable not only because of its low utilization but also its propagation characteristics. The network, which uses the TV frequency bands, can span up to 100 km [13].

B. CONCEPT OF OPERATION AND SYSTEM ARCHITECTURE

The TV frequency bands are fragmented into channels, and some channels are occupied by registered transmitters or incumbents within an area [13]. Other unoccupied channels are available for WRAN transmission, and spectrum allocation is carried out in real-time as spectrum availability varies with time. The system architecture has cognitive mechanisms, which use real-time information to make active frequency selection while preventing interference with incumbents [13]. The frequency agility capability is an important feature of CR due to the time-varying spectrum availability.

The entities in the network are known as the base station (BS) or customer premise equipment (CPE). The BS is required to meet regulations for protection of the incumbents and provides access to a regional database of incumbents [13]. Both the BS

and CPEs utilize cognitive radio techniques, geolocation functions and spectrum-sensing processes to detect occupants in the TV bands [13].

The BS controls the medium access to all associated CPEs within an IEEE 802.22 cell. The downstream medium access from BS to CPE is time-division multiplexed. The upstream transmissions from CPE to BS are shared by CPEs using orthogonal frequency-division multiple access (OFDMA). Each BS and CPE has a 48-bit medium access control (MAC) address for authentication purposes. The BS MAC address is part of the superframe control header (SCH) and is broadcast periodically. Each WRAN device also periodically broadcasts its device identification number and serial number.

C. SPECTRUM MANAGER AND SPECTRUM-SENSING AUTOMATON

The spectrum manager and spectrum-sensing automaton are the two entities, which control the SSF.

The spectrum manager (SM) in the BS plays a central role in the network architecture as it holds a global perspective of the spectrum availability within its coverage area. It retrieves information from the database and collects scanning results from the SSF of CPEs. This information is combined with pre-existing policies and regulations to aid in managing the channel lists, scheduling and coexistence functionalities [11]. The SM also gathers geolocation information of the BS and all associated CPEs before carrying out the assignment of channels to the CPEs.

The spectrum-sensing automaton (SSA) present in each device conducts both in-band and out-of-band sensing when required. In-band sensing is carried out during initialization of the device, pre-association of CPE to BS, change in operating channel, or during assigned in-band quiet periods. In-band quiet periods are assigned time intervals at which in-band spectrum-sensing is performed. The out-of-band sensing is conducted only when the device is not transmitting.

D. BACKUP AND CANDIDATE CHANNEL SETS

The SM manages the channel lists and assigns the channels to the following states: (1) disallowed, (2) operating, (3) backup, (4) candidate, (5) protected, and (6)

unclassified. All channel states are exclusive to each other except when the self-coexistence mechanism is active [13]. The two channel states which are of interest are "backup" and "candidate." The backup channel set contains backup channels, which are ready to be used in the event that interference is detected in the operating channel. The candidate channel set contains candidate channels, which are monitored for some time and are evaluated to be possible backup channels.

The channel states are constantly updated and stored at the SM. The SM creates priorities for channels in the backup and candidate channel sets based on the spectrum etiquette rule [13]. This rule aims to minimize channel collision probability and maximize channel selection pool among WRAN neighboring cells by taking into consideration of the channel sets used in neighboring cells.

E. GEOLOCATION

There are two geolocation mechanisms used in the IEEE standard 802.22, namely satellite-based and terrestrial-based geolocation [13]. Satellite-based geolocation is mandatory since all BS and CPEs are required to share their location before transmission is allowed to occur [13]. Terrestrial-based geolocation is an option to locate a CPE based on distance measurement between CPE and BS, or CPE and reference CPEs. These two mechanisms are available to localize the CPEs [5].

The geolocation information allows the BS and CPEs to access the regional database information such as location of the licensed users, their transmission power, operating frequencies and schedules [13].

F. SPECTRUM-SENSING TECHNIQUES

Several sensing techniques and their individual performance are described in Annex C of IEEE 802.22 Standard. Sensing techniques are possible implementations of the SSF [13]. There are two types of sensing, blind-sensing and feature sensing. Blind-sensing does not require any features of a specific signal, while feature sensing requires the features of a specific signal type. The sensing techniques can be categorized as fine-sensing or coarse-sensing. Fine-sensing techniques allow signal detection at a specified

signal power level, while coarse-sensing techniques do not guarantee signal detection for specified signal power levels [13].

1. Blind-Sensing Techniques

The three types of blind-sensing techniques are energy detector, eigenvalue-based, and multi-resolution. They are all coarse-sensing techniques. The energy detector is the simplest and has the lowest computational cost but is subject to noise uncertainty. The eigenvalue-based technique is dependent on both SNR and the signal statistical properties; hence, more time is needed to improve the performance of detection. The multi-resolution technique allows for a configurable frequency window for either faster but less accurate sensing or slower but more accurate sensing.

2. Signal-Specific Sensing Techniques

The signal-specific sensing techniques can be classified into the following categories: (1) matched filtering, (2) spectral correlation, (3) cyclostationary, and (4) statistical covariance, which are all coarse-sensing techniques.

The matched filtering techniques provide the best performance if there is complete knowledge of the received signal. The a priori information can be a signature sequence or pilot symbol of the specific signal type. The spectral correlation is similar to the matched filtering, except that the correlation is conducted in the spectral domain. The cyclostationary method is able to perform in low SNR conditions, but the computational cost is high. The statistical covariance method does not require a priori information of the signal [15] and has an advantage over matched filtering and spectral correlation.

VI. ADAPTIVE LOCALIZATION

A summary of CR capability in IEEE 802.22 CRN was discussed in Chapter V. Since IEEE 802.22 is the first standard to fully integrate the CR concept in a wireless network [2], the required functions to support CRNs in 4G networks would be adopted from IEEE 802.22 and included in the proposed adaptive localization methodology discussed in this chapter.

The motivation of the proposed adaptive localization methodology in this chapter is to locate a 4G-CR target using an external wireless sensor network. A number of related works are discussed. The adaptive localization methodology consists of (1) enhanced cooperative spectrum sensing (ECSS) with active monitoring of channels-of-interest and (2) localization through iterative, non-linear least-squares methods with a Kalman filter from [16]. The first part of the methodology is a modification of the cooperative spectrum-sensing function in [5] and [16]. The second part of the methodology is adopted from the localization method used in [16].

A. OBJECTIVE

In a 4G network such as LTE-advanced or WiMAX 2, the unused channels are available for the commercial, public safety, and military communities [3]. The Defense Advanced Research Projects Agency (DARPA) is exploring the wireless adaptive node network (WANN) project to attain significant gains in throughput via cognitive radios [2]. 4G-CRs will play a pivotal role in the 4G network because they are able to employ spectrum overlay, or opportunistic spectrum access, to achieve spectrum efficiency and flexibility. The applications of 4G-CR include optimization of 4G networks internally and interoperability in heterogeneous communications networks of different service providers and radio standards [2].

The 4G-CRs can be utilized as primary and secondary users in a CRN. The primary users (PUs) are the authorized devices in the network in the specific area, while secondary users (SUs) are allowed to use the spectrum in an opportunistic manner without causing interference with the primary users. In an era of cyber warfare, an

adversary can exploit a group of 4G-CRs after they have been registered as SUs in the network. This adversary can send manipulated information to the BS or misuse the network for harmful purposes.

The localization of 4G-CR signal is challenging due to changes in spatial and frequency components with time. Current localization methods are not sufficient to adapt and continuously track the CR signal.

The objective of the thesis is to employ an external wireless sensor network to locate the target 4G-CR using adaptive localization method.

B. RELATED WORK

The references [5] and [16] are the most relevant papers in terms of adaptive localization. In [5], the extended semi-range based (ESRB) algorithm was proposed to detect and localize a cognitive radio. The four aspects of the algorithm are (1) cooperative spectrum-sensing, (2) spectrum environment mapping, (3) localization through an iterative, non-linear least-squares method, and (4) position refinement [5]. Firstly, each sensor conducts spectrum-sensing by using the energy detection method for each channel. Then the decision making sensor, or decision maker (DM), collects all spectrum-sensing results for data fusion and produce a spectral environment map in real-time. The DM checks the geolocation database and eliminates PUs based on the spectral information; hence, the SUs of interest remain. These SUs are localized, and their positions together with their operating frequency are recorded. The spectrum-sensing cycles are repeated, and the newly obtained positions of SUs are correlated to previous positions to achieve more precise positioning. The SUs are tracked by their positions and operating frequency channels.

While the ESRB algorithm is able to track the spatial and frequency changes [5], there are some weaknesses inherent in the method. The algorithm does not allow SUs to have overlapping paths, so that their moving positions can be correlated between consecutive spectrum-sensing cycles. Furthermore, this means the method cannot support a large number of SUs which have paths that overlap with one another. There is also

some knowledge required that the SU is moving. The DM also temporarily loses track of the SU if the SU is unable to find a channel to occupy.

A more efficient scheme where the Kalman filter is incorporated into the ESRB algorithm in [5] is described in [16]. The results show an improvement in estimating the trajectory of the CR over time.

C. ADAPTIVE LOCALIZATION OF COGNITIVE RADIO IN COGNITIVE RADIO NETWORK (CRN)

The 4G network is assumed to be a CRN with the same cognitive radio capability in the IEEE 802.22 WRAN since both networks utilize the opportunistic spectrum access (OSA) method. The main adopted CR functions from IEEE 802.22 and challenges of a 4G CRN are discussed. The adaptive localization method is conceptualized based on these inputs.

1. Adopted CR Functions from IEEE 802.22 For 4G CRN

The spectrum-sensing functions of BS and SUs are to be similar to those described in IEEE 802.22. Within a 4G CRN cell, the spectrum manager in the BS plays a central role and manages all frequency channels among the PUs and SUs.

Similar to IEEE 802.22, the SUs in 4G CRN periodically scan the spectrum for both backup and candidate channel sets and update the BS. The backup channels allow the SUs to switch channels without disruption to their operation. The spectrum-sensing automaton in each 4G CRN device allows both in-band sensing and out-of-band sensing, where in-band sensing occurs at pre-allocated time slots, and out-of-band sensing occurs when the device is not transmitting.

The network cell prepares for smooth transition in channel changes by keeping channel sets consisting of backup channels and candidate channels. These channel sets are constantly updated after every spectrum-sensing cycle. The SM prioritizes the channels in the channel sets based on the spectrum etiquette rule [13] so as to maximize the channel selection pool among neighboring CRN cells.

Since the locations of the BS and SUs are critical for obtaining accurate geolocation database information, the 4G CRN supports two geolocation mechanisms, namely satellite-based and terrestrial-based. Satellite-based geolocation is mandatory, while terrestrial-based geolocation serves as a backup and ad-hoc option for localization of SUs.

The wide range of spectrum-sensing technique in IEEE 802.22 is also allowed in the 4G CRN.

The SUs establish connection with the BS and provide the necessary information such as location and transmission power. The BS in turn provides the information on the licensed users and the spectrum used.

2. Challenges and Issues of A 4G CRN

The main challenges and issues of locating a 4G-CR in a 4G CRN are (1) mobility of SUs, (2) frequent changes in channel, and (3) high amount of traffic.

One challenge is that in a 4G network, the mobile phone and wireless devices are always mobile. For a cyber warfare threat, it is possible that the target is either moving or stationary.

Since the 4G devices are always moving, the occupied channels change when the devices move from one cell to another. The spectral map within a CRN cell is frequently updated for occupied and unoccupied channels.

Unlike the TV spectrum in which IEEE 802.22 operates, the 4G communications network spectrum are expected to be almost fully occupied and there are limited available channels to be used as backup and candidate channels. This may not be a disadvantage as explained in the adaptive localization method.

3. Proposed Adaptive Localization Methodology

The 4G-CR is capable of frequently changing its spatial and spectral parameters with time. A localization method for 4G-CR requires localization techniques which can anticipate the change in channel occupancy by the adversary.

The adaptive localization methodology presented in this thesis consists of the following parts: (1) enhanced cooperative spectrum sensing (ECSS) with active monitoring of channels-of-interest and (2) localization through an iterative, non-linear least-squares method with a Kalman filter [16].

Similar to the cooperative spectrum-sensing in [5], the DM carries out data fusion from each sensor's spectrum-sensing result to gain a global perspective of the network cell. The DM then produces a spectral map of the network coverage area within the cell. Cooperative spectrum-sensing is required to overcome physical and environmental problems such as multipath fading, non-line-of-sight communications and hidden nodes as mentioned in [17] and [18]. Based on the information gathered from multiple sensors, the cooperative spectrum-sensing technique allows the DM to carry out three functions: (1) identify occupied and unoccupied channels, (2) eliminate channels occupied by PUs by checking the database, and (3) store occupied channels by SUs. In this case, it is assumed that the DM in the wireless sensor network has access to the primary network's geolocation database so that it can determine if the detected user is a primary or secondary user. The ECSS includes a fourth function to monitor the unoccupied channels, which are available for selection as backup or candidate channels.

In a regular cooperative spectrum-sensing cycle, the entire spectrum is scanned, and the first three functions are carried out. In the ECSS technique, there are two types of sensing cycles, namely the full spectrum and monitored channels. The full spectrum scan is a search on all channels on the entire spectrum for incumbents. The monitored channels scan is a search on channels of interest only. When the enhanced cooperative sensing technique is used, the first spectrum-sensing cycle is a full spectrum scan which carries out the four functions mentioned above. The channels to be monitored are the channels occupied by SUs, backup channels and candidate channels. Subsequent spectrum-sensing cycles monitor these channels instead of the full spectrum.

This ECSS technique is advantageous over the cooperative spectrum-sensing technique in [5] because it does not carry out full spectrum scans at each sensing cycle. This greatly reduces the sensing cycle period and allows localization to be carried in

shorter periods. This provides more localization information and is more effective for moving targets.

Another advantage of ECSS is that it is able to track a target more efficiently if the target frequently changes its channel usage. By monitoring the smaller pool of channels, the ECSS is able to quickly identify a new incumbent in these channels and carry out localization of the signal.

The localization of the signals in [16] was verified to be effective for moving targets and is used as part of the adaptive localization method.

VII. CONCLUSION

The objectives of the thesis were (1) to conduct the error analysis for the three proposed TDOA localization methods in [8] and (2) to propose strategies for adaptive localization of 4G-CR. The error analysis of the TDOA localization methods was conducted and the results were analyzed. While the TDOA localization methods in [8] proved to have good error performance, the localization of the 4G-CR cannot solely rely on these conventional localization methods due to the dynamic changes in spatial, frequency and temporal parameters of the signal. The adaptive localization methodology was proposed and discussed in Chapter VI.

A. SUMMARY OF RESULTS

In the error analysis of the TDOA localization method, the localization error was found to be directly proportional to the sensor differential-distance error (or TDOA error) and sensor-position error.

It was predicted that the greater the sensor altitude, the better the localization error would be; however, results showed that there was no such effect. It is to be noted that the Matlab simulation did not take into account the obstruction to the line-of-sight communications in an urbanized environment. The variable with the largest effect on localization error was the TDOA error. The variable with the least effect was the altitude of the sensor. Although the altitudes of sensors do not lead to a large impact on the emitter-position error, it is predicted that they may pose a problem in practical applications in a highly urbanized environment. It was concluded that the four-sensor system has a better performance than the three-sensor system; although, the improvement in performance is not significant.

Due to the dynamic behavior of 4G-CR, the current localization methods are not sufficient to localize the 4G-CR. The proposed adaptive localization method for 4G-CR takes into consideration the changes in spatial, frequency and temporal aspects of the 4G-CR signals. In particular, the ECSS is an improvement to the cooperative spectrum-sensing technique in [5].

B. RECOMMENDATIONS

The localization error was concluded to be most affected by the TDOA error. Since the TDOA error is dependent on the accuracy of TDOA algorithms, future work is required to improve the algorithms in [8].

The localization-error analysis was conducted based on passive and static sensors, including hovering drones; however, the error analysis can be extended for drones moving up to 160 km/h [19].

The challenges of the cognitive radio system are constantly evolving due to demands of remaining stealthy and high utilization of the RF spectrum. The methodology for adaptive localization of cognitive radios, where an external wireless sensor network is used to localize the secondary user target, was described. For faster sensing time, the existing secondary users can be used to detect the secondary user target.

The current method of spectrum overlay, or opportunistic spectrum access, where SUs use the unoccupied channels, may not be sufficient for the future high demands of the 4G network spectrum. Spectrum underlay can be used, and localization of the underlay system is another challenge.

APPENDIX

Matlab Codes:

(1) Version 1 – Using 3 sensors to find worst case of emitter position error

```
%% (1) Initialize constants and variables
sym speedofLight;
speedofLight = 3e8; %meters/sec
sym earthRadius;
earthRadius = 6378e3; %mean equatorial radius in meters

% number of sensors
numofSensors = xlsread('input2.xlsx','constants','B1');
% number of emitters
numofEmitters = xlsread('input2.xlsx','constants','B2');
% uncertainty of distance between sensors - start limit
sensorDistErrorMin = xlsread('input2.xlsx','constants','B3');
% uncertainty of distance between sensors - end limit
sensorDistErrorMax = xlsread('input2.xlsx','constants','B4');
% uncertainty of distance between sensors - increment between limits
sensorDistErrorInc = xlsread('input2.xlsx','constants','B5');
% uncertainty of sensor position error - min limit
sensorPosErrorMin = xlsread('input2.xlsx','constants','B6');
% uncertainty of sensor position error - max limit
sensorPosErrorMax = xlsread('input2.xlsx','constants','B7');
% uncertainty of sensor position error - increment between limits
sensorPosErrorInc = xlsread('input2.xlsx','constants','B8');

%% (2) Find and save positions of emitter and sensors from GPS coordinates

% Read GPS coordinates of emitter and sensors
GPS_posEmitterTable = readtable('input2.xlsx','Sheet','GPSposEmitter');
GPS_posSensorTable = readtable('input2.xlsx','Sheet','GPSposSensor');
GPS_posEmitterArray = table2array(GPS_posEmitterTable);

% Convert latitude,longtitude to x,y,z coordinates
posEmitterTable = zeros(3,numofEmitters);
posSensorTable = zeros(3,numofSensors);
posEmitterTable = latLong2xyz(GPS_posEmitterTable, numofEmitters, earthRadius);
posSensorTable = latLong2xyz(GPS_posSensorTable, numofSensors, earthRadius);
posEmitterArray = table2array(posEmitterTable);
posSensorArray = table2array(posSensorTable);
```

```
%% (3) Iteratively obtain matrix A, and find max RMS of emitterPosError for each
emitter, each sensorDistError

%Initialize variables
sensorDistError_rowSize = 1+uint8((sensorDistErrorMax -
sensorDistErrorMin)/sensorDistErrorInc)
maxRmsResult = zeros(sensorDistError_rowSize,numofEmitters);
sensorPosError_rowSize = (1+uint8((sensorPosErrorMax -
sensorPosErrorMin)/sensorPosErrorInc))
sensorPosMaxRMSemitterResult =
zeros(sensorPosError_rowSize*sensorDistError_rowSize,numofEmitters);
XYmatrix = zeros(3,3);
rowPos = 0;

for EP=1:numofEmitters

   currEmitterPos = posEmitterArray(:,EP);
   currGPSEmitterPos = GPS_posEmitterArray(:,EP);

   for sensorDistError = sensorDistErrorMin:sensorDistErrorInc:sensorDistErrorMax
      sensorDistError_currRow = 1+uint8((sensorDistError -
sensorDistErrorMin)/sensorDistErrorInc);

      for sensorPosError = sensorPosErrorMin:sensorPosErrorInc:sensorPosErrorMax
         sensorPosError_currRow = 1+uint8((sensorPosError -
sensorPosErrorMin)/sensorPosErrorInc);

         % generate A, where A = rate of change of TDOA_ij w.r.t. x or y or z
         A = zeros(4,3);
         A = TDOArateofChange (speedofLight, earthRadius, currGPSEmitterPos,
currEmitterPos, posSensorArray, numofSensors, sensorPosError);

%% (4) for 8 combinations of TDOAerrorVector (u), iteratively solve emitterPosError
vector v

         %initialize
         combination = 2^4; %num of combinations
         emitterPosErrorResult = zeros(combination,3);
         rmsEmitterPosErrorResult = zeros(combination,1);
         meanSqEmitterPosErrorResult = zeros(combination,1);
         TDOAerrorVectorResult = zeros(combination,3+1);
         count = 1;
```

```
        %find 16 combinations of TDOA error vector, since 2^4=16
        TDOAerror = sensorDistError/speedofLight;
        for a = -1:2:1
           for b = -1:2:1
              for c = -1:2:1
                 for d = -1:2:1
                 % generate the TDOA error vector
                 TDOAerrorVector = TDOAerror.*[a; b; c; 1];
                 TDOAerrorVector(4,1) = d*sensorPosError; %altitude error of emitter

                 % Modified least square method
                 deltaXY = findDeltaXY (A,TDOAerrorVector);
                 emitterPosError = findDeltaZ(A,TDOAerrorVector,deltaXY);

                 % find RMS of emitter position error, which is ||v||
                 rmsEmitterPosErrorResult(count,1) = RMS(emitterPosError);

                 % find and store max RMS of emitter position error for current value of
                 % current value of TDOA error and each value of
                 % sensorPosError
                 if (rmsEmitterPosErrorResult(count,1)>
sensorPosMaxRMSemitterResult((sensorDistError_currRow-1) *
sensorPosError_rowSize + sensorPosError_currRow,EP))
                    sensorPosMaxRMSemitterResult((sensorDistError_currRow-1) *
sensorPosError_rowSize + sensorPosError_currRow,EP) =
rmsEmitterPosErrorResult(count,1);
                 end
                  count = count+1;%next combination of TDOA error vector
                 end %d
              end %c
           end %b
        end %a

        % find and store max RMS of emitter position error for
        % current value of TDOA error
        if (sensorPosMaxRMSemitterResult((sensorDistError_currRow-1) *
sensorPosError_rowSize + sensorPosError_currRow,EP)>
maxRmsResult(sensorDistError_currRow,EP))
           maxRmsResult(sensorDistError_currRow,EP) =
sensorPosMaxRMSemitterResult((sensorDistError_currRow-1) *
sensorPosError_rowSize + sensorPosError_currRow,EP);
        end
      end %sensorPosError
   end %sensorsDistError
end %numofEmitters
```

(2) Version 2 – Using 3 sensors to find emitter position error with uniformly distributed variables

```
%% (1) Initialize constants and variables

format long; %display long fixed-decimal format
sym speedofLight;
speedofLight = 3e8; %meters/sec
sym earthRadius;
earthRadius = 6378e3; %mean equatorial radius in meters

% number of sensors
numofSensors = xlsread('input2.xlsx','constants','B1');
% number of emitters
numofEmitters = xlsread('input2.xlsx','constants','B2');
% uncertainty of distance between sensors - start limit
sensorDistErrorMin = xlsread('input2.xlsx','constants','B3');
% uncertainty of distance between sensors - end limit
sensorDistErrorMax = xlsread('input2.xlsx','constants','B4');
% uncertainty of distance between sensors - increment between limits
sensorDistErrorInc = xlsread('input2.xlsx','constants','B5');
% uncertainty of sensor position error - min limit
sensorPosErrorMin = xlsread('input2.xlsx','constants','B6');
% uncertainty of sensor position error - max limit
sensorPosErrorMax = xlsread('input2.xlsx','constants','B7');
% uncertainty of sensor position error - increment between limits
sensorPosErrorInc = xlsread('input2.xlsx','constants','B8');

%% (2) Find and save positions of emitter and sensors from GPS coordinates
% Read GPS coordinates of emitter and sensors
GPS_posEmitterTable = readtable('input2.xlsx','Sheet','GPSposEmitter');
GPS_posSensorTable = readtable('input2.xlsx','Sheet','GPSposSensor');
GPS_posEmitterArray = table2array(GPS_posEmitterTable);

% Convert latitude,longtitude to x,y,z coordinates
posEmitterTable = zeros(3,numofEmitters);
posSensorTable = zeros(3,numofSensors);
posEmitterTable = latLong2xyz(GPS_posEmitterTable, numofEmitters, earthRadius);
posSensorTable = latLong2xyz(GPS_posSensorTable, numofSensors, earthRadius);
posEmitterArray = table2array(posEmitterTable);
posSensorArray = table2array(posSensorTable);
```

```
%% (3) Iteratively obtain matrix A, and find max RMS of emitterPosError for each
emitter, each sensorDistError

%Initialize variables
sensorDistError_rowSize = 1+uint8((sensorDistErrorMax -
sensorDistErrorMin)/sensorDistErrorInc);
maxRmsResult = zeros(sensorDistError_rowSize,numofEmitters);
sensorPosError_rowSize = (1+uint8((sensorPosErrorMax -
sensorPosErrorMin)/sensorPosErrorInc));
sensorPosMaxRMSemitterResult =
zeros(sensorPosError_rowSize*sensorDistError_rowSize,numofEmitters);
XYmatrix = zeros(3,3);
rowPos = 0;
sensorDistErrorMatrix = zeros(3,numofEmitters);%analysis purpose
sensorPosErrorMatrix = zeros(3,numofSensors*numofEmitters); %analysis purpose
altErrorMatrix = zeros(1,numofEmitters); %analysis purpose
TDOAerrorVector = ones(4,1);

for EP=1:numofEmitters
   %emitter x,y,z coordinates and GPS coordinates
   currEmitterPos = posEmitterArray(:,EP);
   currGPSEmitterPos = GPS_posEmitterArray(:,EP);

   %uniform random variable sensorDistError
   sensorDistError = findSensorDistError (sensorDistErrorMin, sensorDistErrorMax);

   % uniform random variable matrix sensorPosError
   sensorPosError = findSensorPosError (numofSensors, sensorPosErrorMin,
sensorPosErrorMax);

    % generate A, where A = rate of change of TDOA_ij w.r.t. x or y or z
    A = TDOArateofChange (speedofLight, earthRadius, currGPSEmitterPos,
currEmitterPos, posSensorArray, numofSensors, sensorPosError);

%% (4) for values of TDOAerrorVector (u), iteratively solve emitterPosError vector v

        %initialize
        emitterPosErrorResult = zeros(8,3);
        rmsEmitterPosErrorResult = zeros(8,1);
        meanSqEmitterPosErrorResult = zeros(8,1);
        TDOAerrorVectorResult = zeros(8,3+1); %LWS: (8,3) 30Apr
        count = 1;
```

```
        % generate the TDOA error vector
        TDOAerrorVector([1:3],1) = sensorDistError./speedofLight; %x,y,z
        altError = findAltError(sensorPosErrorMin, sensorPosErrorMax); %h
        TDOAerrorVector(4,1) = altError;

                % Modified least square method
                deltaXY = findDeltaXY (A,TDOAerrorVector);
                emitterPosError = findDeltaZ(A,TDOAerrorVector, deltaXY);

                %store emitterPosError for each 8 combinations of TDOA
                %error vector
                emitterPosErrorResult(1,[1,2,3]) = transpose(emitterPosError);

                % find RMS of emitter position error, which is ||v||
                rmsEmitterPosErrorResult(1,1) = RMS(emitterPosError);

                % find Mean squared error of v
                % find and store max RMS of emitter position error for
                % current value of TDOA error and each value of
                % sensorPosError
                if (rmsEmitterPosErrorResult(1,1)>
sensorPosMaxRMSemitterResult(1,EP))
                    sensorPosMaxRMSemitterResult(1,EP) =
rmsEmitterPosErrorResult(1,1);
                end

        % find and store max RMS of emitter position error for
        % current value of TDOA error
        if (sensorPosMaxRMSemitterResult(1,EP)> maxRmsResult(1,EP))
           maxRmsResult(1,EP) = sensorPosMaxRMSemitterResult(1,EP);
        end

end %numofEmitters
```

(3) Version 3 – Using 4 sensors to find emitter position error with uniformly distributed variables

```
%% (1) Initialize constants and variables

sym speedofLight;
speedofLight = 3e8; %meters/sec
sym earthRadius;
earthRadius = 6378e3; %mean equatorial radius in meters

% number of sensors
numofSensors = xlsread('input3.xlsx','constants','B1');
% number of emitters
numofEmitters = xlsread('input3.xlsx','constants','B2');
% uncertainty of distance between sensors - start limit
sensorDistErrorMin = xlsread('input3.xlsx','constants','B3');
% uncertainty of distance between sensors - end limit
sensorDistErrorMax = xlsread('input3.xlsx','constants','B4');
% uncertainty of distance between sensors - increment between limits
sensorDistErrorInc = xlsread('input3.xlsx','constants','B5');
% uncertainty of sensor position error - min limit
sensorPosErrorMin = xlsread('input3.xlsx','constants','B6');
% uncertainty of sensor position error - max limit
sensorPosErrorMax = xlsread('input3.xlsx','constants','B7');
% uncertainty of sensor position error - increment between limits
sensorPosErrorInc = xlsread('input3.xlsx','constants','B8');

%% (2) Find and save positions of emitter and sensors from GPS coordinates
% Read GPS coordinates of emitter and sensors
GPS_posEmitterTable = readtable('input3.xlsx','Sheet','GPSposEmitter');
GPS_posSensorTable = readtable('input3.xlsx','Sheet','GPSposSensor');
GPS_posEmitterArray = table2array(GPS_posEmitterTable);

% Convert latitude,longtitude to x,y,z coordinates
posEmitterTable = zeros(3,numofEmitters);
posSensorTable = zeros(3,numofSensors);
posEmitterTable = latLong2xyz(GPS_posEmitterTable, numofEmitters, earthRadius);
posSensorTable = latLong2xyz(GPS_posSensorTable, numofSensors, earthRadius);
posEmitterArray = table2array(posEmitterTable);
posSensorArray = table2array(posSensorTable);
```

```
%% (3) Iteratively obtain matrix A, and find max RMS of emitterPosError for each
emitter, each sensorDistError

%Initialize variables
sensorDistError_rowSize = 1+uint8((sensorDistErrorMax -
sensorDistErrorMin)/sensorDistErrorInc); %15may
maxRmsResult = zeros(sensorDistError_rowSize,numofEmitters);
sensorPosError_rowSize = (1+uint8((sensorPosErrorMax -
sensorPosErrorMin)/sensorPosErrorInc));%09jul
sensorPosMaxRMSemitterResult =
zeros(sensorPosError_rowSize*sensorDistError_rowSize,numofEmitters);
XYmatrix = zeros(3,3);
rowPos = 0;

for EP=1:numofEmitters

   currEmitterPos = posEmitterArray(:,EP);
   currGPSEmitterPos = GPS_posEmitterArray(:,EP);

   for sensorDistError = sensorDistErrorMin:sensorDistErrorInc:sensorDistErrorMax
      sensorDistError_currRow = 1+uint8((sensorDistError -
sensorDistErrorMin)/sensorDistErrorInc);

      for sensorPosError = sensorPosErrorMin:sensorPosErrorInc:sensorPosErrorMax
         sensorPosError_currRow = 1+uint8((sensorPosError -
sensorPosErrorMin)/sensorPosErrorInc);

         % generate A, where A = rate of change of TDOA_ij w.r.t. x or y or z
         A = zeros(4,3);
         A = TDOArateofChangeVer2 (speedofLight, earthRadius, currGPSEmitterPos,
currEmitterPos, posSensorArray, numofSensors, sensorPosError);

%% (4) for 8 combinations of TDOAerrorVector (u), iteratively solve emitterPosError
vector v

         %initialize
         combination = 2^4; %num of combinations
         emitterPosErrorResult = zeros(combination,3);
         rmsEmitterPosErrorResult = zeros(combination,1);
         meanSqEmitterPosErrorResult = zeros(combination,1);
         TDOAerrorVectorResult = zeros(combination,3+1);
         count = 1;
```

```
        %find 16 combinations of TDOA error vector, since 2^4=16
        TDOAerror = sensorDistError/speedofLight;
        for a = -1:2:1
           for b = -1:2:1
              for c = -1:2:1
                 for d = -1:2:1
                 % generate the TDOA error vector
                 TDOAerrorVector = TDOAerror.*[a; b; c; 1];
                 TDOAerrorVector(4,1) = d*sensorPosError; %altitude error of emitter

                 % Modified least square method
                 deltaXY = findDeltaXY (A,TDOAerrorVector);
                 emitterPosError = findDeltaZ(A,TDOAerrorVector,deltaXY);

                 % find RMS of emitter position error, which is ||v||
                 rmsEmitterPosErrorResult(count,1) = RMS(emitterPosError);

                 % find and store max RMS of emitter position error for
                 % current value of TDOA error and each value of
                 % sensorPosError
                 if (rmsEmitterPosErrorResult(count,1)>
sensorPosMaxRMSemitterResult((sensorDistError_currRow-1) *
sensorPosError_rowSize + sensorPosError_currRow,EP))
                    sensorPosMaxRMSemitterResult((sensorDistError_currRow-1) *
sensorPosError_rowSize + sensorPosError_currRow,EP) =
rmsEmitterPosErrorResult(count,1);
                 end
                  count = count+1;%next combination of TDOA error vector
                 end %d
              end %c
           end %b
        end %a

        % find and store max RMS of emitter position error for
        % current value of TDOA error
        if (sensorPosMaxRMSemitterResult((sensorDistError_currRow-1) *
sensorPosError_rowSize + sensorPosError_currRow,EP)>
maxRmsResult(sensorDistError_currRow,EP))
           maxRmsResult(sensorDistError_currRow,EP) =
sensorPosMaxRMSemitterResult((sensorDistError_currRow-1) *
sensorPosError_rowSize + sensorPosError_currRow,EP);
        end
      end %sensorPosError
   end %sensorsDistError
   end %numofEmitters
```

THIS PAGE INTENTIONALLY LEFT BLANK

LIST OF REFERENCES

[1] Mobile communications, International Telecommunication Union. (2013, Aug. 20). International Telecommunication Union. [Online]. Available: http://www.itu.int/ITU-D/tech/MobileCommunications/IMT_INTRODUCING/IMT_2G3G4G.html

[2] M. J. Kaur, M. Uddin and H. K. Verma. (2012, Feb. 1). Role of Cognitive Radio on 4G Communications: A Review. Journal of Emerging Trends in Computing and Information Sciences. [Online]. 3(2). pp. 272–276. Available: http://www.cisjournal.org/journalofcomputing/Download_February_pdf_22.aspx

[3] J. E. Gunn. (2007, Jun.). SDR Market Study Task 5: The Cognitive Radio Market. Jim Gunn Consultancy. Richardson, TX. [Online]. Available: http://groups.winnforum.org/Market_Studies_Public

[4] Definition of Software Defined Radio (SDR) and Cognitive Radio System (CRS). (2015). International Telecommunication Union. [Online]. Available: http://www.itu.int/pub/R-REP-SM.2152-2009

[5] A. Adams, "Source localization in a cognitive radio environment consisting of frequency and spatial mobility," M.S. thesis, Dept. Elect. Eng., Naval Postgraduate School., Monterey, CA, 2011.

[6] S. Sun, Y. Ju, and Y. Yamao, "Overlay cognitive radio OFDM system for 4G cellular networks," *IEEE Wireless Communications,* vol. 20, no. 2, pp. 68–73, Apr. 2013.

[7] H. Celebi and H. Arslan, "Cognitive Positioning Systems," *IEEE Transactions on Wireless Communications*, vol. 6, pp. 4475–4483, 2007.

[8] T. Ha, W. Su and R. Romero, "Technical report for National Reconnaissance office – Comprehensive Study of Strength and Weakness of 4G Cognitive Radio to aid in designing effective signal localization and tracking methods," Dept. Elect. Eng., Naval Postgraduate School, Monterey, CA, Tech. Rep. NRO-TR-PART-A, Jul. 2014

[9] T. T. Ha and R. C. Robertson, "Geostationary Satellite Navigation Systems," *IEEE Transactions on Aerospace and Electronic Systems*, vol. AES-23, pp. 247–254, 1987.

[10] K. C. Ho and Y. T. Chan, "Solution and performance analysis of geolocation by TDOA," *IEEE Transactions on Aerospace and Electronic Systems*, vol. 29, pp. 1311–1322, 1993.

[11] F. Gustafsson and F. Gunnarsson, “Positioning using time-difference of arrival measurements,” *IEEE International Conference on Acoustics, Speech, and Signal Processing,* 2003, pp. 553–556 vol.6.

[12] Xiaomei Qu and Lihua Xie, “Source localization by TDOA with random sensor position errors — part I: Static sensors,” *15th International Conference on Information Fusion (FUSION),* Singapore, 2012, pp. 48–53.

[13] *IEEE Standard for Information Technology— Local and Metropolitan Area Networks— Specific Requirements— Part 22: Cognitive Wireless RAN Medium Access Control (MAC) and Physical Layer (PHY) Specifications: Policies and Procedures for Operation in the TV Bands*, IEEE Standard 802.22, 2011.

[14] Li Chen, Tengyi Zhang and D. H. K. Tsang, “SALT: Sensing enAbled localization and tracking for geolocation database in TV white space,” *9th International Wireless Communications and Mobile Computing Conference,* 2013, pp. 712–717.

[15] Yonghong Zeng and Ying-Chang Liang, “Covariance based signal detections for cognitive radio,” *2nd IEEE International Symposium on New Frontiers in Dynamic Spectrum Access Networks,* 2007, pp. 202–207.

[16] A. Adams, M. Tummala, J. McEachen and J. Scrofani, “Source localization and tracking in a cognitive radio environment consisting of frequency and spatial mobility,” *7th International Conference on Signal Processing and Communication Systems*, 2013, pp. 1–6.

[17] I. F. Akyildiz, B. F. Lo, R. Balakrishnan. (2010, Dec. 11). Cooperative spectrum sensing in cognitive radio networks: A survey. Physical Communication. [Online]. 4(1). pp. 40–62. Available: http://dl.acm.org/citation.cfm?id=2295264

[18] G. Ganesan and Ye Li, “Cooperative spectrum sensing in cognitive radio networks,” *First IEEE International Symposium on New Frontiers in Dynamic Spectrum Access Networks,* 2005, pp. 137–143.

[19] Jansen, B. (2015, Feb. 16). FAA unveils drone rules; Obama orders policy for agencies. USA Today [Online]. Available: http://www.usatoday.com/story/news/2015/02/15/faa-drone-rule/23440469/

INITIAL DISTRIBUTION LIST

1. Defense Technical Information Center
   Ft. Belvoir, Virginia

2. Dudley Knox Library
   Naval Postgraduate School
   Monterey, California